

# 1 Speciation in the face of gene flow within the toothed whale superfamily Delphinoidea

2  
3 Michael V Westbury<sup>1\*</sup>, Andrea A. Cabrera<sup>1</sup>, Alba Rey-Iglesia<sup>1</sup>, Binia De Cahsan<sup>1</sup>, Stefanie  
4 Hartmann<sup>2</sup>, Eline D Lorenzen<sup>1\*</sup>

- 5 1. GLOBE Institute, University of Copenhagen, Øster Voldgade 5-7, Copenhagen,  
6 Denmark  
7 2. Institute of Biochemistry and Biology, University of Potsdam, Karl-Liebknecht-Str.  
8 24-25, Potsdam, Germany

9 \* Corresponding authors: m.westbury@sund.ku.dk, elinelorenzen@sund.ku.dk

## 10 11 **Abstract**

12  
13 Understanding speciation is a central aspect in Biology. The formation of new species  
14 was once thought to be a simple bifurcation process. However, recent advances in genomic  
15 resources now provide the opportunity to investigate the role of post-divergence gene flow in  
16 the speciation process. The diversification of lineages in the presence of gene flow appears  
17 almost paradoxical. However, with enough time and in the presence of incomplete physical  
18 and/or ecological barriers to gene flow, speciation can and does occur. Speciation without  
19 complete isolation seems especially likely to occur in highly mobile, wide-ranging marine  
20 species, such as cetaceans, which face limited geographic barriers. The toothed whale  
21 superfamily Delphinoidea represents a good example to further explore speciation in the  
22 presence of interspecific gene flow. Delphinoidea consists of three families (Delphinidae,  
23 Phocoenidae, and Monodontidae) and within all three families, contemporary interspecific  
24 hybrids have been reported. Here, we utilise publicly available genomes from nine species,  
25 representing all three Delphinoidea families, to investigate signs of post-divergence gene  
26 flow across their genomes, and to address the speciation processes that led to the diversity  
27 seen today within the superfamily. We use a multifaceted approach including: (i)  
28 phylogenetics, (ii) the distribution of shared derived alleles, and (iii) demography-based. We  
29 find that the divergence and evolution of lineages in Delphinoidea did not follow a simple  
30 bifurcating pattern, but were much more complex. Our results indicate multiple, ancestral  
31 gene flow events within and among families, which occurred millions of years after initial  
32 divergence.

## 33 34 **Introduction**

35  
36 The formation of new species involves the divergence of lineages through  
37 reproductive isolation. Such isolation can initially occur in allopatry (geographical isolation)  
38 or in sympatry (biological/ecological isolation). Over time, these barriers are maintained and  
39 strengthened, ultimately leading to the formation of new species (Norris and Hull, 2012).  
40 While allopatric speciation requires geographical isolation plus time, sympatric speciation  
41 often requires a broader and more complicated set of mechanisms (Turelli et al., 2001). These  
42 mechanisms mostly rely on ecologically-mediated natural selection. Parapatric speciation, on

43 the other hand, encompasses intermediate scenarios of partial, but incomplete, physical  
44 restrictions to gene flow leading to speciation.

45

46 Through the analysis of whole-genome datasets, the detection of post-divergence gene  
47 flow between distinct species is becoming more commonplace (Árnason et al., 2018; Barlow  
48 et al., 2018; Westbury et al., 2020), demonstrating that speciation is much more complex than  
49 a simple bifurcating process (Campbell and Poelstra, 2018; Feder et al., 2012). Speciation is  
50 not an instantaneous process, but requires tens of thousands to millions of generations to  
51 achieve complete reproductive isolation (Butlin and Smadja, 2018; Coyne and Orr, 2004; Liu  
52 et al., 2014). The duration it takes to reach this isolation may be especially long in highly  
53 mobile marine species, such as cetaceans, due to a relative lack of geographic barriers in the  
54 marine realm, and therefore high potential for secondary contact and gene flow (Árnason et  
55 al., 2018).

56

57 The apparent inability to undergo allopatric speciation in marine species has been  
58 termed the marine-speciation paradox (Bierne et al., 2003). However, over the past decade,  
59 genomic studies have provided some insights into how speciation can occur within cetaceans  
60 (Árnason et al., 2018; Moura et al., 2020). For example, in killer whales (*Orcinus orca*) it has  
61 been proposed that initial phases of allopatry may have led to the accumulation of ecological  
62 differences between populations, which strengthened population differences even after they  
63 came into secondary contact (Foote et al., 2011; Foote and Morin, 2015). However, whether  
64 these initial phases of allopatry caused the divergence, or whether speciation occurred purely  
65 in sympatry, remains debated (Moura et al., 2015). Yet these two hypotheses are not  
66 necessarily mutually exclusive. Instead, differentiation in parapatry, encompassing features of  
67 both allopatric and sympatric speciation, may have been key in the evolutionary history of  
68 cetaceans.

69

70 The toothed whale superfamily Delphinoidea represents an interesting opportunity to  
71 further explore speciation in the presence of putative interspecific gene flow. The root of  
72 Delphinoidea has been dated to 19 million years ago (Ma) (95% CI 19.73 - 18.26 Ma)  
73 (McGowen et al., 2020) and has given rise to three families: (i) Delphinidae, the most  
74 species-rich family, which comprises dolphins and ‘black-fish’ (such as killer whales and  
75 pilot whales (*Globicephala spp.*)); (ii) Phocoenidae, commonly known as porpoises; and (iii)  
76 Monodontidae, which comprises two surviving lineages, belugas (*Delphinapterus leucas*) and  
77 narwhals (*Monodon monoceros*).

78

79 Delphinoidea is of particular interest, as contemporary interspecific hybrids have been  
80 reported within all three families (Delphinidae: (Espada et al., 2019; Miyazaki et al., 1992;  
81 Silva et al., 2005); Phocoenidae: (Willis et al., 2004) Monodontidae: (Skovrind et al., 2019).  
82 However, these hybrids represent recent hybridization events that occurred long after species  
83 divergence, and their contribution to the parental gene pools is mostly unknown. The  
84 presence of more ancient introgressive hybridization events between families, and during the  
85 early radiations of these families, has yet to be investigated. With the rapid increase of  
86 genomic resources for cetaceans, and in particular for species within Delphinoidea, we are

87 presented with the ideal opportunity to investigate post-divergence gene flow between  
88 lineages, furthering our understanding of speciation processes in cetaceans.

89

90 Here, we utilise publicly available whole-genome data from nine species of  
91 Delphinoidea, representing all three families, to investigate signs of post-divergence gene  
92 flow across their genomes. Our analyses included five Delphinidae (killer whale, Pacific  
93 white-sided dolphin (*Lagenorhynchus obliquidens*), long-finned pilot whale (*Globicephala*  
94 *melas*), bottlenose dolphin (*Tursiops truncatus*), Indo-Pacific bottlenose dolphin (*T.*  
95 *aduncus*)); two Phocoenidae (harbour porpoise (*Phocoena phocoena*), finless porpoise  
96 (*Neophocaena phocaenoides*)); and two Monodontidae (beluga, narwhal). Moreover, we  
97 compare their species-specific genetic diversity and demographic histories, and explore how  
98 species abundances may have played a role in interspecific hybridisation over the last two  
99 million years.

100

## 101 **Results and discussion**

102

### 103 **Detecting gene flow**

104 To assess the evolutionary relationships across the genomes of the nine Delphinoidea  
105 species investigated, we computed non-overlapping sliding-window maximum-likelihood  
106 phylogenies of four different window sizes in RAxML (Stamatakis, 2014). These analyses  
107 resulted in 43,207 trees (50 kilobase (kb) windows), 21,387 trees (100 kb windows), 3,705  
108 trees (500 kb windows), and 1,541 trees (1 megabase (Mb) windows) (Fig. 1, Supplementary  
109 Fig. S1, Supplementary table S1). The 50 kb windows retrieved a total of 96 unique  
110 topologies, 100 kb windows retrieved 47 unique topologies, 500 kb windows retrieved a total  
111 of 16 unique topologies, and 1 Mb windows retrieved a total of 15 unique topologies.  
112 Regardless of window size, we retrieve consensus support for the species tree previously  
113 reported using target-sequence capture (McGowen et al., 2020). However, when considering  
114 the smallest window size (50 kb), we find a considerable proportion of trees (up to 76%) with  
115 an alternative topology to the known species tree (Fig. 1A). These alternative topologies  
116 could be due to incomplete lineage sorting (ILS) or interspecific gene flow (Leaché et al.,  
117 2014). Moreover, the higher prevalence of this pattern in the 50 kb windows (for example,  
118 21% of windows show an alternative topology in the 1 Mb dataset (Fig. 1B)), may indicate  
119 that inconsistencies in topology are caused by ancient, rather than recent, events.

120 We explored whether the large number of phylogenetic discrepancies in the 50kb  
121 windows could be linked to the GC content (%GC) of the windows. Discrepancies could  
122 arise, as elevated levels of GC content can result from higher levels of GC-Biased Gene  
123 Conversion (gBGC) in regions with higher levels of recombination (Lartillot, 2013). When  
124 binning windows into either high, medium, or low levels of GC content, the most common  
125 topologies are consistent, but with slight differences in overall values (Supplementary table  
126 S2). This result suggests that the topological discrepancies are not arising purely due to GC-  
127 content linked biases and recombination rate.

128

129 To investigate whether the alternative topologies could simply be explained by ILS,  
130 or whether a combination of ILS and gene flow was a more probable cause, we ran

131 Quantifying Introgression via Branch Lengths (QuIBL) (Edelman et al., 2019) on every  
132 twentieth tree from the 50 kb sliding-window analysis (Supplementary table S3), as well as  
133 on a dataset that contained trees constructed using 20 kb windows with a 1Mb slide  
134 (Supplementary table S4). As we did not recover any large number of phylogenetic  
135 discrepancies between families, we were only able to look at the potential cause of  
136 discrepancies in the Delphinidae family. Our QuIBL analyses suggest that the different  
137 retrieved topologies cannot be explained by ILS alone, but a combination of both ILS and  
138 gene flow.

139

140 To further explore potential gene flow while taking ILS into account, we applied D-  
141 statistics. D-statistics uses a four-taxon approach  $[[[H1, H2], H3], \text{Outgroup}]$  to uncover the  
142 differential distribution of shared derived alleles, which may represent gene flow between  
143 either H1/H3 or H2/H3. Here we used baiji (*Lipotes vexillifer*) as the outgroup, and alternated  
144 ingroup positions based on the consensus topology. We find that 85 out of 86 tests show  
145 signs of gene flow within and between families (Supplementary table S5), suggesting the  
146 evolutionary history of Delphinoidea was more complex than a simple bifurcating process.

147

148 Due to the inability of the four-taxon D-statistics approach to detect the direction of  
149 gene flow, as well as whether gene flow events may have occurred between ancestral  
150 lineages, we used D-foil. D-foil enables further characterization of the D-statistics results,  
151 which may be particularly relevant, given the complex array of gene flow putatively present  
152 within Delphinoidea. D-foil uses a five-taxon approach  $[[H1, H2] [H3, H4], \text{Outgroup}]$  and a  
153 system of four independent D-statistics in a sliding-window fashion to uncover (i) putative  
154 gene flow events, (ii) donor and recipient lineages, and (iii) whether gene flow events  
155 occurred between a distantly related lineage and the ancestor of two sister lineages, which is  
156 indicative of ancestral-lineage gene flow. However, due to the input topology requirements of  
157 D-foil, we were only able to investigate gene flow between families, and not within families,  
158 using this analysis. Hence, we tested for gene flow between Delphinidae/Phocoenidae,  
159 Delphinidae/Monodontidae, and Monodontidae/Phocoenidae.

160

161 The D-foil results underscore the complex pattern of post-divergence gene flow  
162 between families indicated by the D-statistics. We find support for interfamilial gene flow  
163 events between all nine species investigated, to varying extents (Supplementary table S6).  
164 This could reflect multiple episodes of gene flow between all investigated species.  
165 Alternatively, the pattern could reflect ancient gene flow events between the ancestors of H1-  
166 H2 and H3-H4 (in the topology  $[[H1, H2] [H3, H4], \text{Outgroup}]$ ), with differential inheritance  
167 of the admixed loci in subsequent lineages. Such ancestral gene flow events have previously  
168 been shown to lead to false positives between species pairs using D-statistics (Moodley et al.,  
169 2020). A further putative problem with these results can be seen when implementing D-foil  
170 on the topology  $[[\text{Delphinidae}, \text{Delphinidae}], [\text{Monodontidae}, \text{Phocoenidae}], \text{Outgroup}]$ . We  
171 find the majority of windows support a closer relationship between Delphinidae (ancestors of  
172 H1 and H2) and Monodontidae (H3), as opposed to the species tree. If this result is correct, it  
173 suggests the input topology was incorrect, implying that Delphinidae and Monodontidae are  
174 sister lineages, as opposed to Phocoenidae and Monodontidae. However, this contrasts with

175 the family topology of [Delphinidae, [Phocoenidae, Monodontidae]] retrieved in our  
176 phylogenetic analyses (Fig. 1) and reported by others (McGowen et al., 2020; Steeman et al.,  
177 2009). Instead, we suggest our result reflects the limited ability of D-foil to infer gene flow  
178 between these highly divergent lineages.

179

180 False positives and potential biases in D-statistics and D-foil can arise due to a  
181 number of factors including (i) ancestral population structure, (ii) introgression from  
182 unsampled and/or extinct ghost lineages, (iii) differences in relative population size of  
183 lineages or in the timing of gene flow events, (iv) different evolutionary rates or sequencing  
184 errors between H1 and H2, and (v) gene flow between ancestral lineages (Moodley et al.,  
185 2020; Slatkin and Pollack, 2008; Zheng and Janke, 2018). These issues are important to  
186 consider when interpreting our results, as the deep divergences of lineages suggest there were  
187 probably a number of ancestral gene flow events, as well as gene flow events between now-  
188 extinct lineages, that may bias results.

189

### 190 **Cessation of gene flow**

191 To further elucidate the complexity of interspecific gene flow within Delphinoidea,  
192 we implemented F1 hybrid PSMC (hPSMC) (Cahill et al., 2016). This method creates a  
193 pseudo-diploid sequence by merging pseudo-haploid sequences from two different genomes,  
194 which in our case represents two different species. The variation in the interspecific pseudo-  
195 F1 hybrid genome cannot coalesce more recently than the emergence of reproductive  
196 isolation between the two parental species, and the method can therefore be used to infer  
197 when gene flow between species ceased.

198

199 When considering the uppermost limit of when gene flow ended (equating to the most  
200 ancient date) and the lower confidence interval of each divergence date (equating to the most  
201 recent date), the majority of comparisons (29/36) show that post-divergence gene flow  
202 occurred for >50% of the post-divergence branch length (Fig. 2, Supplementary results). This  
203 finding suggests that reaching complete reproductive isolation in Delphinoidea was a slow  
204 process. The occurrence of post-divergence gene flow long after initial divergence may  
205 reflect the ability of these cetacean species to travel long distances, and the lack of significant  
206 geographical barriers in the marine environment. Alternatively, if geographic barriers did  
207 lead to the initial divergences, the pattern could reflect recontact before complete isolation.

208

209 Despite our finding of long-term gene flow in the majority of comparisons, our results  
210 suggest gene flow ceased more rapidly within the Delphinidae family, relative to within  
211 Phocoenidae and Monodontidae (Fig. 2). Only three out of ten pairwise comparisons (killer  
212 whale vs Indo-Pacific white-sided dolphin, killer whale vs long-finned pilot whale, and  
213 bottlenose dolphin vs Indo-Pacific bottlenose dolphin), showed gene flow at >50% of the  
214 branch length post divergence. The remaining seven comparisons showed gene flow along  
215 48% - 24% of the post-divergence branch length. This finding may reflect the inability of  
216 hPSMC to detect low levels of migration until the present day, leading to large estimated  
217 intervals around the time point at which gene flow ceased.

218

219 Simulations have shown that in the presence of as few as 1/10,000 migrants per  
220 generation, hPSMC suggests continued gene flow. However, this does not happen with a rate  
221 of less than  $\sim 1/100,000$  migrants per generation. Rather, in the latter case, the exponential  
222 increase in  $N_e$  of the pseudo-hybrid genome, which is used to infer the date at which gene  
223 flow ceased between the parental individuals, becomes a more gradual transition, leading to a  
224 larger estimated time interval (Cahill et al., 2016). Within Delphinidae, we observe a  
225 corresponding, less pronounced increase in  $N_e$  in the pseudo-hybrids, suggestive of  
226 continued, but very low migration rates (Supplementary results). This finding suggests that  
227 gene flow within Delphinidae may have continued for longer than shown by hPSMC, which  
228 may not be sensitive enough to detect the low rates of recent gene flow. Furthermore,  
229 persistent gene flow is supported by confirmed fertile contemporary hybrids between some of  
230 our study species; for example, bottlenose dolphins can produce fertile offspring with both  
231 Indo-Pacific bottlenose dolphins (Gridley et al., 2018) and Pacific white-sided dolphins  
232 (Crossman et al., 2016; Miyazaki et al., 1992). Either way, our hPSMC results within and  
233 between all three families show a consistent pattern of long periods of interspecific migration  
234 in Delphinoidea, some lasting up to more than ten million years post divergence.

235

236 We further investigated the robustness of our hPSMC results to the inclusion or  
237 exclusion of repeat regions in the pseudodiploid genome. We compared the hPSMC results  
238 when including and removing repeat regions for three independent species pairs of varying  
239 levels of phylogenetic distance. These included a shallow divergence (bottlenose and Indo-  
240 Pacific bottlenose dolphins), medium divergence (beluga and narwhal), and deep divergence  
241 (bottlenose dolphin and beluga) (Supplementary figs S2 - S4). For all species pairs, results  
242 showed that the pre-divergence  $N_e$  is almost identical, and the exponential increase in  $N_e$  is  
243 just slightly more recent when removing the repeat regions compared to when repeat regions  
244 are included. This gives us confidence that the inclusion of repeats did not greatly influence  
245 our results.

246

## 247 **Interspecific hybridisation**

248

249 Making inferences as to what biological factors lead to interspecific hybridisation is  
250 challenging, as many variables may play a role. One hypothesis is that interspecific  
251 hybridization may occur at a higher rate during periods of low abundance, when a given  
252 species encounters only a limited number of conspecifics (Crossman et al., 2016; Edwards et  
253 al., 2011; Westbury et al., 2019). When considering species that have not yet undergone  
254 sufficient divergence, preventing their ability to hybridise, individuals may mate with a  
255 closely-related species, instead of investing energy in finding a rarer conspecific mate.

256

257 To explore the relationship between susceptibility to interspecific hybridisation and  
258 population size, we calculated the level of genome-wide genetic diversity for each species, as  
259 a proxy for their population size (Fig. 3A). Narwhal, killer whale, beluga and long-finned  
260 pilot whale have the lowest diversity levels, and should therefore be more susceptible to  
261 interspecific hybridization events. A beluga/narwhal hybrid has been reported (Skovrind et  
262 al., 2019), as has hybridisation between long-finned and short-finned pilot whales (Miralles et

263 al., 2016). However, hybrids between species with high genetic diversity, including harbour  
264 porpoise (Willis et al., 2004), Indo-Pacific bottlenose dolphin (Baird et al., 2012), and  
265 bottlenose dolphin (Espada et al., 2019; Herzing and Johnson, 1997) have also been  
266 reported, suggesting genetic diversity alone is not a good proxy for susceptibility to  
267 hybridisation.

268

269 To investigate whether interspecific gene flow took place during past periods of low  
270 population size, we estimated changes in intraspecific genetic diversity through time (Fig.  
271 3B-D). The modeled demographic trajectories, using a Pairwise Sequentially Markovian  
272 Coalescent model (PSMC), span the past two million years. We could therefore assess the  
273 relationship for the three species pairs, where the interval for the cessation of gene flow was  
274 contained within this period: harbour/finless porpoise (Phocoenidae), beluga/narwhal  
275 (Monodontidae), and bottlenose/Indo-Pacific bottlenose dolphin (Delphinidae) (Fig. 2).

276

277 In the harbour porpoise, we observe an increase in effective population size ( $N_e$ )  
278 beginning ~1 Ma, the rate of which increases further ~0.5 Ma (Fig. 3C). The timing of  
279 expansion overlaps the period during which gene flow with the finless porpoise ceased (~1.1  
280 - 0.5 Ma, Fig. 2), suggesting gene flow between the two species occurred when population  
281 size in the harbour porpoise was lower. We observe a similar pattern in belugas; an increase  
282 in  $N_e$  ~1 Ma, relatively soon after the proposed cessation of gene flow with narwhals ~1.8 -  
283 1.2 Ma (Fig. 3D). An increase in  $N_e$  may coincide with an increase in relative abundance,  
284 which would increase the number of potential conspecific mates, and in turn reduce the level  
285 of interspecific gene flow. Although we are unable to test the direction and levels of gene  
286 flow between these species pairs, we expect a relative reduction of gene flow into the more  
287 abundant species. A relative reduction of such events would in turn lessen genomic signs of  
288 interspecific gene flow, despite its occurrence.

289

290 We observe a different pattern in the bottlenose/Indo-Pacific bottlenose dolphins. In  
291 the previous examples, we find a relatively low population size when gene flow was ongoing,  
292 and only in one of the two hybridizing species. In the dolphins, we find a relatively high  
293 population size during the period of gene flow in both species;  $N_e$  declines ~1 - 0.5 Ma,  
294 coinciding with the putative end of gene flow ~1.2 - 0.4 Ma. The decline in  $N_e$  could either  
295 reflect a decline in abundance, or a loss of connectivity between the two species. In the latter,  
296 we expect levels of intraspecific diversity (and thereby inferred  $N_e$ ) to decline with the  
297 cessation of gene flow, even if absolute abundances did not change. This is indeed suggested  
298 by our data, which shows both species undergoing the decline simultaneously, indicative of a  
299 common cause.

300

301 Seven of the nine Delphinoidea genomes investigated show a similar pattern of a  
302 rapid decline in  $N_e$  starting ~150 - 100 thousands of years ago (kya) (Fig. 3B-D; the  
303 exceptions are Pacific white-sided dolphin and narwhal). This concurrent decline could  
304 represent actual population declines across species, or, alternatively, simultaneous reductions  
305 in connectivity among populations within each species. Based on similar PSMC analyses, a  
306 decline in  $N_e$  at this time has also been reported in four baleen whale species (Árnason et al.,

307 2018). Although this could reflect demographic factors, such as the loss of population  
308 connectivity, the unique life histories, distributions, and ecology of these cetacean species  
309 suggests that decreased population connectivity is unlikely to have occurred simultaneously  
310 across all studied species.

311

312 Rather, the species-wide pattern may reflect climate-driven environmental change.  
313 The period of 150 - 100 kya overlaps with the onset of the last interglacial, when sea levels  
314 increased to levels as high, if not higher, than at present (Polyak et al., 2018), and which may  
315 have had a marine-wide effect on population sizes. A similar marine-wide effect has been  
316 observed among baleen whales and their prey species in the Southern and North Atlantic  
317 Oceans during the Pleistocene-Holocene climate transition (12-7 kya) (Cabrera et al., 2018).  
318 These results lend support to the ability of marine-wide environmental shifts to drive changes  
319 in population sizes across multiple species.

320

321 Although currently speculative based on our demographic results, we suggest recent  
322 species-wide declines may have facilitated the resurgence of hybridization between the nine  
323 Delphinoidea species analysed here. If hybridisation did increase, species may already have  
324 been sufficiently differentiated that offspring fertility was reduced. Even if offspring were  
325 fertile, the high level of differentiation between species may have meant hybrids were unable  
326 to occupy either parental niche (Skovrind et al., 2019) and were therefore strongly selected  
327 against. A lack of significant contribution from hybrids to the parental gene pools may be  
328 why we observe contemporary hybrids, despite lacking evidence of this in the hPSMC  
329 analysis.

330

## 331 **Conclusions**

332

333 Allopatric speciation is generally considered the most common mode of speciation, as  
334 the absence of gene flow due to geographical isolation can most easily explain the evolution  
335 of ecological, behavioural, morphological, or genetic differences between populations (Norris  
336 and Hull, 2012). However, our findings suggest that within Delphinoidea, speciation in the  
337 presence of gene flow was commonplace, consistent with sympatric/parapatric speciation, or  
338 allopatric speciation and secondary contact.

339

340 The ability for gene flow events to occur long after initial divergence may also  
341 explain the presence of contemporaneous hybrids between several species. In parapatric  
342 speciation, genetic isolation is achieved relatively early due to geographical and biological  
343 isolation, but species develop complete reproductive isolation relatively slowly, through low  
344 levels of migration or secondary contact events allowing hybridization to continue for an  
345 extended period of time (Norris and Hull, 2012). The prevalence of this mode of speciation in  
346 cetaceans, as suggested by our study and previous genomic analyses (Árnason et al., 2018;  
347 Moura et al., 2020), may reflect the low energetic costs of dispersing across large distances in  
348 the marine realm (Fish et al., 2008; Williams, 1999) and the relative absence of geographic  
349 barriers preventing such dispersal events (Palumbi, 1994). Both factors are believed to be



350 important in facilitating long-distance (including inter-hemispheric and inter-oceanic)  
351 movements in many cetacean species (Stone et al., 1990).

352

353 Our study shows that speciation in Delphinoidea was a complex process and involved  
354 multiple ecological and evolutionary factors. Our results take a step towards resolving the  
355 enormous complexity of speciation through a multifaceted analysis of nuclear genomes.  
356 However, we also uncover difficulties in precisely interpreting some results due to the high  
357 levels of divergence between species included in the analysis. Despite this, we are still able to  
358 form hypotheses about general patterns and major processes we uncovered in our data that we  
359 hope can be addressed as more genomic data and new analyses become available.

360

## 361 **Methods**

362

### 363 **Data collection**

364 We downloaded the assembled genomes and raw sequencing reads from nine toothed  
365 whales from the superfamily Delphinoidea. The data included five Delphinidae: Indo-Pacific  
366 white-sided dolphin (NCBI Biosample: SAMN09386610), Indo-Pacific bottlenose dolphin  
367 (NCBI Biosample: SAMN06289676), bottlenose dolphin (NCBI Biosample:  
368 SAMN09426418), killer whale (NCBI Biosample: SAMN01180276), and long-finned pilot  
369 whale (NCBI Biosample: SAMN11083132); two Phocoenidae: harbour porpoise (Autenrieth  
370 et al., 2018), finless porpoise (NCBI Biosample: SAMN02192673); and two Monodontidae:  
371 beluga (NCBI Biosample: SAMN06216270), narwhal (NCBI Biosample: SAMN10519625).  
372 To avoid biases that may occur when mapping to an ingroup reference (Westbury et al.,  
373 2019), we used the assembled baiji genome (Genbank accession code: GCF\_000442215.1) as  
374 mapping reference in the gene flow analyses. Delphinoidea and the baiji diverged ~24.6 Ma  
375 (95% CI 25.2 - 23.8 Ma) (McGowen et al., 2020).

376

### 377 **Initial data filtering**

378 To determine which scaffolds were most likely autosomal in origin, we identified  
379 putative sex chromosome scaffolds for each genome, and omitted them from further analysis.  
380 We found putative sex chromosome scaffolds in all ten genomes by aligning the assemblies  
381 to the Cow X (Genbank accession: CM008168.2) and Human Y (Genbank accession:  
382 NC\_000024.10) chromosomes. Alignments were performed using satsuma synteny v2.1  
383 (Grabherr et al., 2010) with default parameters. We also removed scaffolds smaller than 100  
384 kb from all downstream analyses.

385

### 386 **Mapping**

387 We trimmed adapter sequences from all raw reads using skewer v0.2.2 (Jiang et al.,  
388 2014). We mapped the trimmed reads to the baiji for downstream gene flow analyses, and to  
389 the species-specific reference genome for downstream demographic history and genetic  
390 diversity analyses using BWA v0.7.15 (Li and Durbin, 2009) and the mem algorithm. We  
391 parsed the output and removed duplicates and reads with a mapping quality lower than 30  
392 with SAMtools v1.6 (Li et al., 2009). Mapping statistics can be found in supplementary tables  
393 S7 and S8.

394

### 395 **Sliding-window phylogeny**

396 For the sliding-window phylogenetic analysis, we created fasta files for all individuals  
397 mapped to the baiji genome using a consensus base call (-dofasta 2) approach in ANGSD  
398 v0.921 (Korneliussen et al., 2014), and specifying the following filters: minimum read depth  
399 of 5 (-mininddepth 5), minimum mapping quality of 30 (-minmapq 30), minimum base  
400 quality (-minq 30), only consider reads that map to one location uniquely (-uniqueonly 1),  
401 and only include reads where both mates map (-only\_proper\_pairs 1). All resultant fasta files,  
402 together with the assembled baiji genome, were aligned, and sites where any individual had  
403 more than 50% missing data were filtered before performing maximum likelihood  
404 phylogenetic analyses in a non-overlapping sliding-window approach using RAxML v8.2.10  
405 (Stamatakis, 2014). We performed this analysis four times independently, specifying a  
406 different window size each time (50 kb, 100 kb, 500 kb, and 1 Mb). We used RAxML with  
407 default parameters, specifying baiji as the outgroup, and a GTR+G substitution model. We  
408 computed the genome-wide majority rule consensus tree for each window size in PHYLIP  
409 (Felsenstein, 2005), with branch support represented by the proportion of trees displaying the  
410 same topology. We simultaneously visualised all trees of the same sized window using  
411 DensiTree (Bouckaert, 2010).

412 We tested whether results may be linked to GC content in the 50kb windows. To do  
413 this, we calculated the GC content for each window and binned the windows into three bins:  
414 The 33% with the lowest levels of GC content, the 33% with intermediate levels, and the  
415 33% with the highest levels of GC content.

416

### 417 **Quantifying Introgression via Branch Lengths (QuIBL)**

418 To test hypotheses of whether phylogenetic discordance between all possible triplets  
419 can be explained by ILS alone, or by a combination of ILS and gene flow, we implemented  
420 QuIBL (Edelman et al., 2019) and two different datasets. The first dataset leveraged the  
421 results of the above 50 kb-window analysis, by taking every twentieth tree from the 50kb  
422 sliding-window analysis and running it through QuIBL. The second dataset was created  
423 specifically for this test, and contained topologies generated from 20 kb windows with a 1  
424 Mb slide using the phylogenetic methods mentioned above. We ran QuIBL specifying the  
425 baiji as the overall outgroup (totaloutgroup), to test either ILS or ILS with gene flow  
426 (numdistributions 2), the number of total EM steps as 50 (numsteps), and a likelihood  
427 threshold of 0.01. We determined significance of gene flow by comparing the BIC1 (ILS  
428 alone) and BIC2 (assuming ILS and gene flow). If BIC2 was lower than BIC1, with a  
429 difference of greater than 10, then we assumed incongruent topologies arose due to both ILS  
430 and gene flow. Triplet topologies supporting the species tree, and those that had <5  
431 alternative topologies were excluded from interpretations.

432

### 433 **D-statistics**

434 To test for signs of gene flow in the face of incomplete lineage sorting (ILS), we ran  
435 D-statistics using all individuals mapped to the baiji genome in ANGSD, using a consensus  
436 base call approach (-doabbababa 2), specifying the baiji sequence as the ancestral outgroup  
437 sequence, and the same filtering as for the fasta file construction with the addition of setting

438 the block size as 1Mb (-blocksize). Significance of the results was evaluated using a block  
439 jackknife approach with the Rscript provided in the ANGSD package.  $|Z| > 3$  was deemed  
440 significant.

441

#### 442 **D-foil**

443 As D-statistics only tests for the presence and not the direction of gene flow, we ran  
444 D-foil (Pease and Hahn, 2015), an extended version of the D-statistics, which is a five-taxon  
445 test for gene flow, making use of all four combinations of the potential D-statistics  
446 topologies. For this analysis, we used the same fasta files constructed above, which we  
447 converted into an mvf file using MVFtools (Pease and Rosenzweig, 2018). We specified the  
448 5-taxon [[H1, H2], [H3, H4], baiji], for all possible combinations, following the species tree  
449 (McGowen et al., 2020) (Fig. 1) and a 100 kb window size. All scaffolds were trimmed to the  
450 nearest 100 kb to avoid the inclusion of windows shorter than 100 kb.

451

#### 452 **Mutation rate estimation**

453 For use in the downstream demographic analyses, we computed the mutation rate per  
454 generation for each species. To do this, we estimated the pairwise distances between all  
455 ingroup species mapped to the baiji, using a consensus base call in ANGSD (-doIBS 2), and  
456 applying the same filters as above, with the addition of only considering sites in which all  
457 individuals were covered (-minInd). The pairwise distances used in this calculation were  
458 those from the closest lineage to the species of interest (Supplementary tables S9 and S10).  
459 The mutation rates per generation were calculated using the resultant pairwise distance as  
460 follows: mutation rate = pairwise distance x generation time / 2 x divergence time.  
461 Divergence times were taken from the full dataset 10-partition AR (mean) values from  
462 McGowen et al. (McGowen et al., 2020) (Supplementary table S10). Generation times were  
463 taken from previously published data (Supplementary table S11).

464

#### 465 **Cessation of gene flow**

466 To estimate when gene flow may have ceased between each species pair, we used the  
467 F1-hybrid PSMC (hPSMC) approach (Cahill et al., 2016). As input we used the haploid  
468 consensus sequences mapped to the baiji that were created for the phylogenetic analyses.  
469 Despite the possibility of producing consensus sequences when mapping to a conspecific  
470 reference genomes, we chose the baiji for all comparisons as previous analyses have shown  
471 the choice of reference genome to not influence the results of hPSMC (Westbury et al.,  
472 2019). We merged the haploid sequences from each possible species pair into pseudo-diploid  
473 sequences using the scripts available in the hPSMC toolsuite. We independently ran each  
474 resultant species pair pseudo-diploid sequences through PSMC, specifying atomic intervals  
475 4+25\*2+4+6. We plotted the results using the average (i) mutation rate per generation and (ii)  
476 generation time for each species pair being tested. From the output of this analysis, we  
477 visually estimated the pre-divergence  $N_e$  of each hPSMC plot (i.e.  $N_e$  prior to the point of  
478 asymptotic increase in  $N_e$ ) to be used as input for downstream simulations. Based on these  
479 empirical results, we ran simulations in ms (Hudson, 2002) using the estimated pre-  
480 divergence  $N_e$ , and various predefined divergence times to find the interval in which gene  
481 flow may have ceased between a given species pair. The time intervals and pre-divergence

482 Ne for each species pair used for the simulations can be seen in supplementary table S12. The  
483 ms commands were produced using the scripts available in the hPSMC toolsuite. We plotted  
484 the simulated and empirical hPSMC results to find the simulations with an asymptotic  
485 increase in Ne closest to, but not overlapping with, the empirical data. The predefined  
486 divergence times of the simulations showing this pattern within 1.5x and 10x of the pre-  
487 divergence Ne were taken as the time interval in which gene flow ceased.

488  
489 We repeated the above analysis for three species pairs bottlenose/Indo-Pacific  
490 bottlenose dolphins, beluga/narwhal, and beluga/bottlenose dolphin, but with an additional  
491 step, where we masked repeat elements of the haploid genomes using bedtools (Quinlan,  
492 2014) and the repeat annotations available on Genbank. Once we masked the repeat elements,  
493 we reran the hPSMC analysis as above.

### 494 495 **Heterozygosity**

496 As a proxy for species-level genetic diversity, we estimated autosome-wide  
497 heterozygosity for each of the nine Delphinoidea species. We estimated autosomal  
498 heterozygosity using allele frequencies (-doSaf 1) in ANGSD (Korneliussen et al., 2014),  
499 taking genotype likelihoods into account (-GL 2) and specifying the same filters as for the  
500 fasta file construction with the addition of adjusting quality scores around indels (-baq 1), and  
501 the subsample filter (-downSample), which was uniquely set for each individual to result in a  
502 20x genome-wide coverage, to ensure comparability between genomes of differing coverage.  
503 Heterozygosity was computed from the output of this using realSFS from the ANGSD  
504 toolsuite and specifying 20 Mb windows of covered sites (-nSites).

### 505 506 **Demographic reconstruction**

507 To determine the demographic histories of all nine species over a two million year  
508 time scale, we ran a Pairwise Sequentially Markovian Coalescent model (PSMC) (Li and  
509 Durbin, 2011) on each diploid genome independently. We called diploid genome sequences  
510 using SAMtools and BCFtools v1.6 (Narasimhan et al., 2016), specifying a minimum quality  
511 score of 20 and minimum coverage of 10. We ran PSMC specifying atomic intervals  
512 4+25\*2+4+6 and performed 100 bootstrap replicates to investigate support for the resultant  
513 demographic trajectories. PSMC outputs were plotted using species-specific mutation rates  
514 and generation times (Supplementary table S11).

### 515 516 **Figure legends:**

517  
518 **Figure 1: Sliding-Window Maximum likelihood trees of nine Delphinoidea species and**  
519 **the baiji.** Simultaneously plotted trees constructed using non-overlapping sliding windows of  
520 (A) 50 kb in length and (B) 1 Mb in length. Black lines show the consensus tree. Grey lines  
521 show individual trees. Numbers on branches show the proportion of windows supporting the  
522 node. Branches without numbers show 100% support. Baiji, killer whale, white-sided  
523 dolphin, pilot whale, harbour porpoise, finless whale, beluga, and narwhal silhouettes: Chris  
524 huh, license CC-BY-SA-3.0 (<https://creativecommons.org/licenses/by-sa/3.0/>). Bottlenose  
525 dolphin silhouette: license Public Domain Dedication 1.0.

526  
527  
528  
529  
530  
531  
532  
533  
534  
535  
536  
537  
538  
539  
540  
541  
542  
543  
544  
545  
546  
547  
548  
549  
550  
551  
552  
553  
554  
555  
556  
557  
558  
559  
560  
561  
562  
563  
564  
565  
566  
567

**Figure 2: Estimated divergence times (dark colour) and time intervals during which gene flow ceased (light colour) between species (A) within families and (B) between families.** Estimated time intervals of when gene flow ceased between species pairs are based on hPSMC results and simulated data. Divergence time estimates are taken from the full dataset 10-partition AR results of McGowen et al 2020.

**Figure 3: Autosome-wide heterozygosity and demographic histories over the last two million years.** (A) Autosome-wide levels of heterozygosity calculated in 20 Mb windows of consecutive bases. (B-D) Demographic history of all studied species within (B) Delphinidae, (C) Phocoenidae, and (D) Monodontidae, estimated using PSMC. Thick coloured lines show the autosome-wide demographic history. Faded lines show bootstrap support values.

### **Acknowledgements**

The work was supported by the Carlsberg Foundation Distinguished Associate Professor Fellowship, grant no CF16-0202, the Villum Fonden Young Investigator Programme, grant no. 13151, and the Independent Research Fund Denmark | Natural Sciences, Forskningsprojekt 1, grant no. 8021-00218B to EDL. AAC was funded by the Rubicon-NWO grant (project 019.183EN.005). We would like to thank all those contributing to the ever-increasing abundance of publicly available genomic resources. Without the availability of such data, our study would not have been possible.

### **Author contributions**

Conceptualization, MVW; Formal analysis, MVW, AAC, AR-I, BDC, SH; Writing – Original Draft MVW; Writing – Review & Editing All authors; Supervision, MVW, EDL; Funding Acquisition, EDL;

568 **References:**

- 569 Árnason Ú, Lammers F, Kumar V, Nilsson MA, Janke A. 2018. Whole-genome sequencing  
 570 of the blue whale and other rorquals finds signatures for introgressive gene flow. *Sci Adv*  
 571 **4**:eaap9873.
- 572 Autenrieth M, Hartmann S, Lah L, Roos A, Dennis AB, Tiedemann R. 2018. High-quality  
 573 whole-genome sequence of an abundant Holarctic odontocete, the harbour porpoise  
 574 (*Phocoena phocoena*). *Mol Ecol Resour* **18**:1469–1481.
- 575 Baird RW, Gorgone AM, McSweeney DJ, Ligon AD, Deakos MH, Webster DL, Schorr GS,  
 576 Martien KK, Salden DR, Mahaffy SD. 2012. Population structure of island-associated  
 577 dolphins: Evidence from mitochondrial and microsatellite markers for common  
 578 bottlenose dolphins (*Tursiops truncatus*) in the main Hawaiian Islands. *Mar Mamm Sci*.  
 579 Barlow A, Cahill JA, Hartmann S, Theunert C, Xenikoudakis G, Fortes GG, Paijmans JLA,  
 580 Rabeder G, Frischauf C, Grandal-d’Anglade A, García-Vázquez A, Murtskhvaladze M,  
 581 Saarma U, Anijalg P, Skrbinšek T, Bertorelle G, Gasparian B, Bar-Oz G, Pinhasi R,  
 582 Slatkin M, Dalén L, Shapiro B, Hofreiter M. 2018. Partial genomic survival of cave  
 583 bears in living brown bears. *Nat Ecol Evol* **2**:1563–1570.
- 584 Bierne N, Bonhomme F, David P. 2003. Habitat preference and the marine-speciation  
 585 paradox. *Proc Biol Sci* **270**:1399–1406.
- 586 Bouckaert RR. 2010. DensiTree: making sense of sets of phylogenetic trees. *Bioinformatics*  
 587 **26**:1372–1373.
- 588 Butlin RK, Smadja CM. 2018. Coupling, Reinforcement, and Speciation. *Am Nat* **191**:155–  
 589 172.
- 590 Cabrera AA, Schall E, Bérubé M, Bachmann L, Berrow S, Best PB, Clapham PJ, Cunha HA,  
 591 Rosa LD, Dias C, Findlay KP, Haug T, Heide-Jørgensen MP, Kovacs KM, Landry S,  
 592 Larsen F, Lopes XM, Lydersen C, Mattila DK, Oosting T, Pace RM, Papetti C, Paspati  
 593 A, Pastene LA, Prieto R, Ramp C, Robbins J, Ryan C, Sears R, Secchi ER, Silva MA,  
 594 Víkingsson G, Wiig Ø, Øien N, Palsbøll PJ. 2018. Strong and lasting impacts of past  
 595 global warming on baleen whale and prey abundance. *bioRxiv*.
- 596 Cahill JA, Soares AER, Green RE, Shapiro B. 2016. Inferring species divergence times using  
 597 pairwise sequential Markovian coalescent modelling and low-coverage genomic data.  
 598 *Philos Trans R Soc Lond B Biol Sci* **371**. doi:10.1098/rstb.2015.0138
- 599 Campbell CR, Poelstra JW. 2018. What is Speciation Genomics? The roles of ecology, gene  
 600 flow, and genomic architecture in the formation of species. *Biol J Linn Soc Lond*  
 601 **124**:561–583.
- 602 Coyne JA, Orr HA. 2004. Speciation. Sinauer Associates Sunderland, MA.
- 603 Crossman CA, Taylor EB, Barrett-Lennard LG. 2016. Hybridization in the Cetacea:  
 604 widespread occurrence and associated morphological, behavioral, and ecological factors.  
 605 *Ecol Evol* **6**:1293–1303.
- 606 Edelman NB, Frandsen PB, Miyagi M, Clavijo B, Davey J, Dikow RB, García-Accinelli G,  
 607 Van Belleghem SM, Patterson N, Neafsey DE, Challis R, Kumar S, Moreira GRP,  
 608 Salazar C, Chouteau M, Counterman BA, Papa R, Blaxter M, Reed RD, Dasmahapatra  
 609 KK, Kronforst M, Joron M, Jiggins CD, McMillan WO, Di Palma F, Blumberg AJ,  
 610 Wakeley J, Jaffe D, Mallet J. 2019. Genomic architecture and introgression shape a  
 611 butterfly radiation. *Science* **366**:594–599.
- 612 Edwards CJ, Suchard MA, Lemey P, Welch JJ, Barnes I, Fulton TL, Barnett R, O’Connell  
 613 TC, Coxon P, Monaghan N, Valdiosera CE, Lorenzen ED, Willerslev E, Baryshnikov  
 614 GF, Rambaut A, Thomas MG, Bradley DG, Shapiro B. 2011. Ancient hybridization and  
 615 an Irish origin for the modern polar bear matriline. *Curr Biol* **21**:1251–1258.
- 616 Espada R, Olaya-Ponzzone L, Haasova L, Martín E, García-Gómez JC. 2019. Hybridization in

617 the wild between *Tursiops truncatus* (Montagu 1821) and *Delphinus delphis* (Linnaeus  
618 1758). *PLoS One* **14**:e0215020.

619 Feder JL, Egan SP, Nosil P. 2012. The genomics of speciation-with-gene-flow. *Trends Genet*  
620 **28**:342–350.

621 Felsenstein J. 2005. PHYLIP (Phylogeny Inference Package) version 3.6.

622 Fish FE, Howle LE, Murray MM. 2008. Hydrodynamic flow control in marine mammals.  
623 *Integr Comp Biol* **48**:788–800.

624 Foote AD, Morin PA. 2015. Sympatric speciation in killer whales? *Heredity* **114**:537–538.

625 Foote AD, Morin PA, Durban JW, Willerslev E. 2011. Out of the Pacific and back again:  
626 insights into the matrilineal history of Pacific killer whale ecotypes. *PLoS*.

627 Grabherr MG, Russell P, Meyer M, Mauceli E, Alföldi J, Di Palma F, Lindblad-Toh K. 2010.  
628 Genome-wide synteny through highly sensitive sequence alignment: Satsuma.  
629 *Bioinformatics* **26**:1145–1151.

630 Gridley T, Elwen SH, Harris G, Moore DM, Hoelzel AR, Lampen F. 2018. Hybridization in  
631 bottlenose dolphins—A case study of *Tursiops aduncus* × *T. truncatus* hybrids and  
632 successful backcross hybridization events. *PLoS One* **13**:e0201722.

633 Herzing DL, Johnsonz CM. 1997. Interspecific interactions between Atlantic spotted  
634 dolphins (*Stenella frontalis*) and bottlenose dolphins (*Tursiops truncatus*) in the  
635 Bahamas 1985-1995. *Aquat Mamm*.

636 Hudson RR. 2002. Generating samples under a Wright–Fisher neutral model of genetic  
637 variation. *Bioinformatics* **18**:337–338.

638 Jiang H, Lei R, Ding S-W, Zhu S. 2014. Skewer: a fast and accurate adapter trimmer for  
639 next-generation sequencing paired-end reads. *BMC Bioinformatics* **15**:182.

640 Korneliussen TS, Albrechtsen A, Nielsen R. 2014. ANGSD: Analysis of Next Generation  
641 Sequencing Data. *BMC Bioinformatics* **15**:356.

642 Lartillot N. 2013. Phylogenetic patterns of GC-biased gene conversion in placental mammals  
643 and the evolutionary dynamics of recombination landscapes. *Mol Biol Evol* **30**:489–502.

644 Leaché AD, Harris RB, Rannala B, Yang Z. 2014. The influence of gene flow on species tree  
645 estimation: a simulation study. *Syst Biol* **63**:17–30.

646 Li H, Durbin R. 2011. Inference of human population history from individual whole-genome  
647 sequences. *Nature* **475**:493–496.

648 Li H, Durbin R. 2009. Fast and accurate short read alignment with Burrows–Wheeler  
649 transform. *Bioinformatics* **25**:1754–1760.

650 Li H, Handsaker B, Wysoker A, Fennell T, Ruan J, Homer N, Marth G, Abecasis G, Durbin  
651 R, 1000 Genome Project Data Processing Subgroup. 2009. The Sequence  
652 Alignment/Map format and SAMtools. *Bioinformatics* **25**:2078–2079.

653 Liu S, Lorenzen ED, Fumagalli M, Li B, Harris K, Xiong Z, Zhou L, Korneliussen TS, Somel  
654 M, Babbitt C, Wray G, Li J, He W, Wang Z, Fu W, Xiang X, Morgan CC, Doherty A,  
655 O’Connell MJ, McNerney JO, Born EW, Dalén L, Dietz R, Orlando L, Sonne C, Zhang  
656 G, Nielsen R, Willerslev E, Wang J. 2014. Population genomics reveal recent speciation  
657 and rapid evolutionary adaptation in polar bears. *Cell* **157**:785–794.

658 McGowen MR, Tsagkogeorga G, Álvarez-Carretero S, Dos Reis M, Struebig M, Deaville R,  
659 Jepson PD, Jarman S, Polanowski A, Morin PA, Rossiter SJ. 2020. Phylogenomic  
660 Resolution of the Cetacean Tree of Life Using Target Sequence Capture. *Syst Biol*  
661 **69**:479–501.

662 Miralles L, Oremus M, Silva MA, Planes S, Garcia-Vazquez E. 2016. Interspecific  
663 Hybridization in Pilot Whales and Asymmetric Genetic Introgression in Northern  
664 Globicephala melas under the Scenario of Global Warming. *PLoS One* **11**:e0160080.

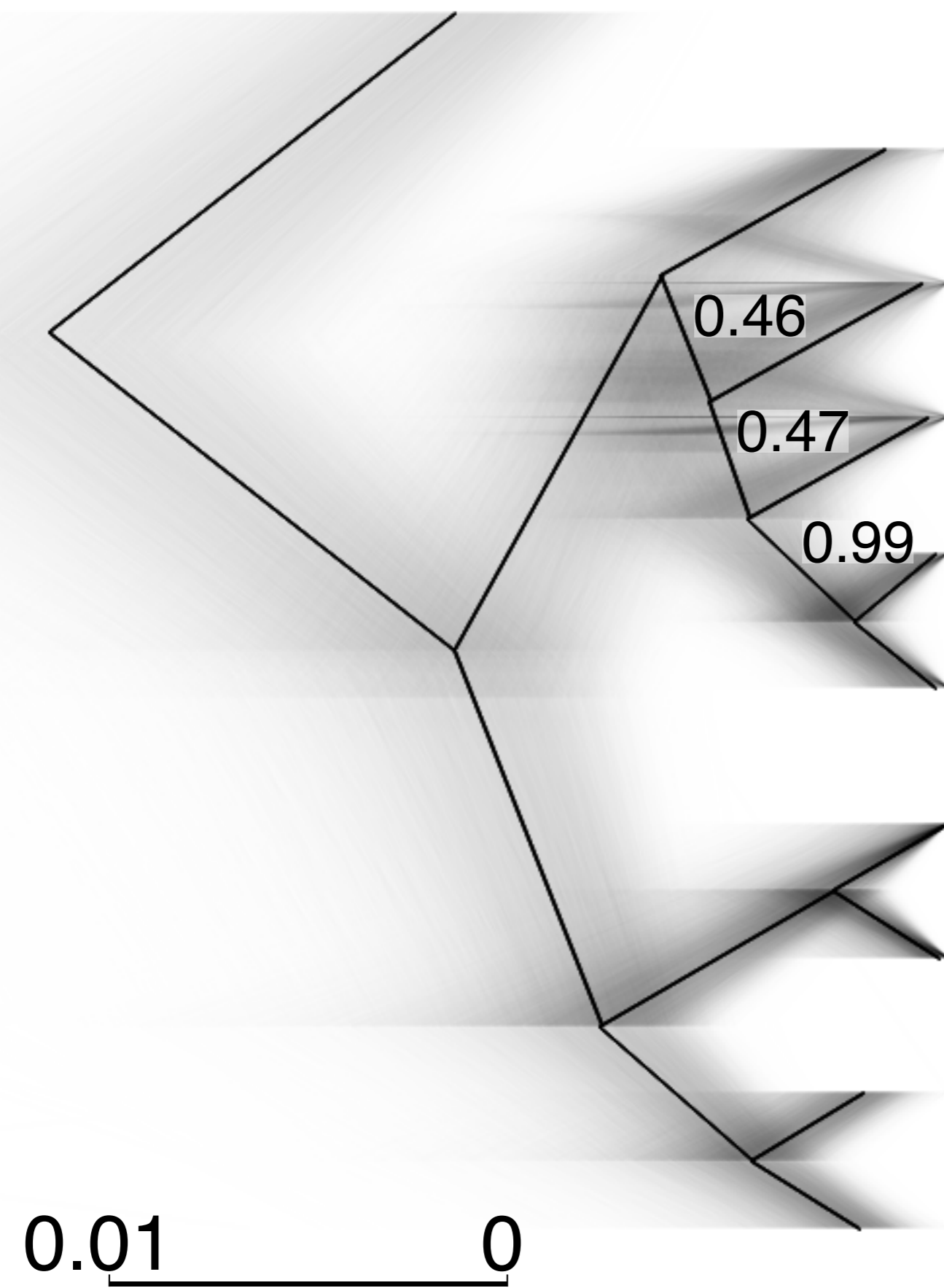
665 Miyazaki N, Hirosaki Y, Kinuta T, Omura H. 1992. Osteological study of a hybrid between  
666 *Tursiops truncatus* and *Grampus griseus*. *Bull Natl Mus Nat Sci Ser B Bot* **18**:79–94.

- 667 Moodley Y, Westbury MV, Russo I-RM, Gopalakrishnan S, Rakotoarivelo A, Olsen R-A,  
668 Prost S, Tunstall T, Ryder OA, Dalén L, Bruford MW. 2020. Interspecific gene flow and  
669 the evolution of specialisation in black and white rhinoceros. *Mol Biol Evol.*  
670 doi:10.1093/molbev/msaa148
- 671 Moura AE, Kenny JG, Chaudhuri RR, Hughes MA. 2015. Phylogenomics of the killer whale  
672 indicates ecotype divergence in sympatry. *Heredity* **114**:48–55.
- 673 Moura AE, Shreves K, Pilot M, Andrews KR, Moore DM, Kishida T, Möller L, Natoli A,  
674 Gaspari S, McGowen M, Chen I, Gray H, Gore M, Culloch RM, Kiani MS, Willson MS,  
675 Bulushi A, Collins T, Baldwin R, Willson A, Minton G, Ponnampalam L, Hoelzel AR.  
676 2020. Phylogenomics of the genus *Tursiops* and closely related Delphininae reveals  
677 extensive reticulation among lineages and provides inference about eco-evolutionary  
678 drivers. *Mol Phylogenet Evol* **146**:106756.
- 679 Narasimhan V, Danecek P, Scally A, Xue Y, Tyler-Smith C, Durbin R. 2016. BCFtools/RoH:  
680 a hidden Markov model approach for detecting autozygosity from next-generation  
681 sequencing data. *Bioinformatics* **32**:1749–1751.
- 682 Norris RD, Hull PM. 2012. The temporal dimension of marine speciation. *Evol Ecol* **26**:393–  
683 415.
- 684 Palumbi SR. 1994. Genetic divergence, reproductive isolation, and marine speciation. *Annu*  
685 *Rev Ecol Syst* **25**:547–572.
- 686 Pease JB, Hahn MW. 2015. Detection and Polarization of Introgression in a Five-Taxon  
687 Phylogeny. *Syst Biol* **64**:651–662.
- 688 Pease JB, Rosenzweig BK. 2018. Encoding Data Using Biological Principles: The  
689 Multisample Variant Format for Phylogenomics and Population Genomics. *IEEE/ACM*  
690 *Trans Comput Biol Bioinform* **15**:1231–1238.
- 691 Polyak VJ, Onac BP, Fornós JJ, Hay C, Asmerom Y, Dorale JA, Ginés J, Tuccimei P, Ginés  
692 A. 2018. A highly resolved record of relative sea level in the western Mediterranean Sea  
693 during the last interglacial period. *Nat Geosci* **11**:860–864.
- 694 Quinlan AR. 2014. BEDTools: The Swiss-Army Tool for Genome Feature Analysis. *Curr*  
695 *Protoc Bioinformatics* **47**:11.12.1–34.
- 696 Silva JM, Silva FJL, Sazima I. 2005. Two presumed interspecific hybrids in the genus  
697 *Stenella* (Delphinidae) in the Tropical West Atlantic. *Aquat Mamm* **31**:468.
- 698 Skovrind M, Castruita JAS, Haile J, Treadaway EC, Gopalakrishnan S, Westbury MV,  
699 Heide-Jørgensen MP, Szpak P, Lorenzen ED. 2019. Hybridization between two high  
700 Arctic cetaceans confirmed by genomic analysis. *Sci Rep* **9**:7729.
- 701 Slatkin M, Pollack JL. 2008. Subdivision in an ancestral species creates asymmetry in gene  
702 trees. *Mol Biol Evol* **25**:2241–2246.
- 703 Stamatakis A. 2014. RAxML version 8: a tool for phylogenetic analysis and post-analysis of  
704 large phylogenies. *Bioinformatics* **30**:1312–1313.
- 705 Steeman ME, Hebsgaard MB, Fordyce RE, Ho SYW, Rabosky DL, Nielsen R, Rahbek C,  
706 Glenner H, Sørensen MV, Willerslev E. 2009. Radiation of extant cetaceans driven by  
707 restructuring of the oceans. *Syst Biol* **58**:573–585.
- 708 Stone G, Florez-Gonzalez L, Katona S. 1990. Whale migration record. *Nature* **346**:705–705.
- 709 Turelli M, Barton NH, Coyne JA. 2001. Theory and speciation. *Trends Ecol Evol* **16**:330–  
710 343.
- 711 Westbury MV, Hartmann S, Barlow A, Preick M, Ridush B, Nagel D, Rathgeber T, Ziegler  
712 R, Baryshnikov G, Sheng G, Ludwig A, Wiesel I, Dalen L, Bibi F, Werdelin L, Heller  
713 R, Hofreiter M. 2020. Hyena paleogenomes reveal a complex evolutionary history of  
714 cross-continental gene flow between spotted and cave hyena. *Science Advances*  
715 **6**:eaay0456.
- 716 Westbury MV, Petersen B, Lorenzen ED. 2019. Genomic analyses reveal an absence of

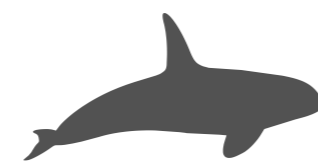


717 contemporary introgressive admixture between fin whales and blue whales, despite  
718 known hybrids. *PLoS One* **14**:e0222004.  
719 Williams TM. 1999. The evolution of cost efficient swimming in marine mammals: limits to  
720 energetic optimization. *Philosophical Transactions of the Royal Society of London*  
721 *Series B: Biological Sciences* **354**:193–201.  
722 Willis PM, Crespi BJ, Dill LM, Baird RW, Hanson MB. 2004. Natural hybridization between  
723 Dall's porpoises (*Phocoenoides dalli*) and harbour porpoises (*Phocoena phocoena*). *Can*  
724 *J Zool* **82**:828–834.  
725 Zheng Y, Janke A. 2018. Gene flow analysis method, the D-statistic, is robust in a wide  
726 parameter space. *BMC Bioinformatics* **19**:10.

727

**A**

Baiji



Killer whale



White-sided dolphin



Pilot whale



Bottlenose dolphin

Indo bottlenose  
dolphin

Harbour porpoise



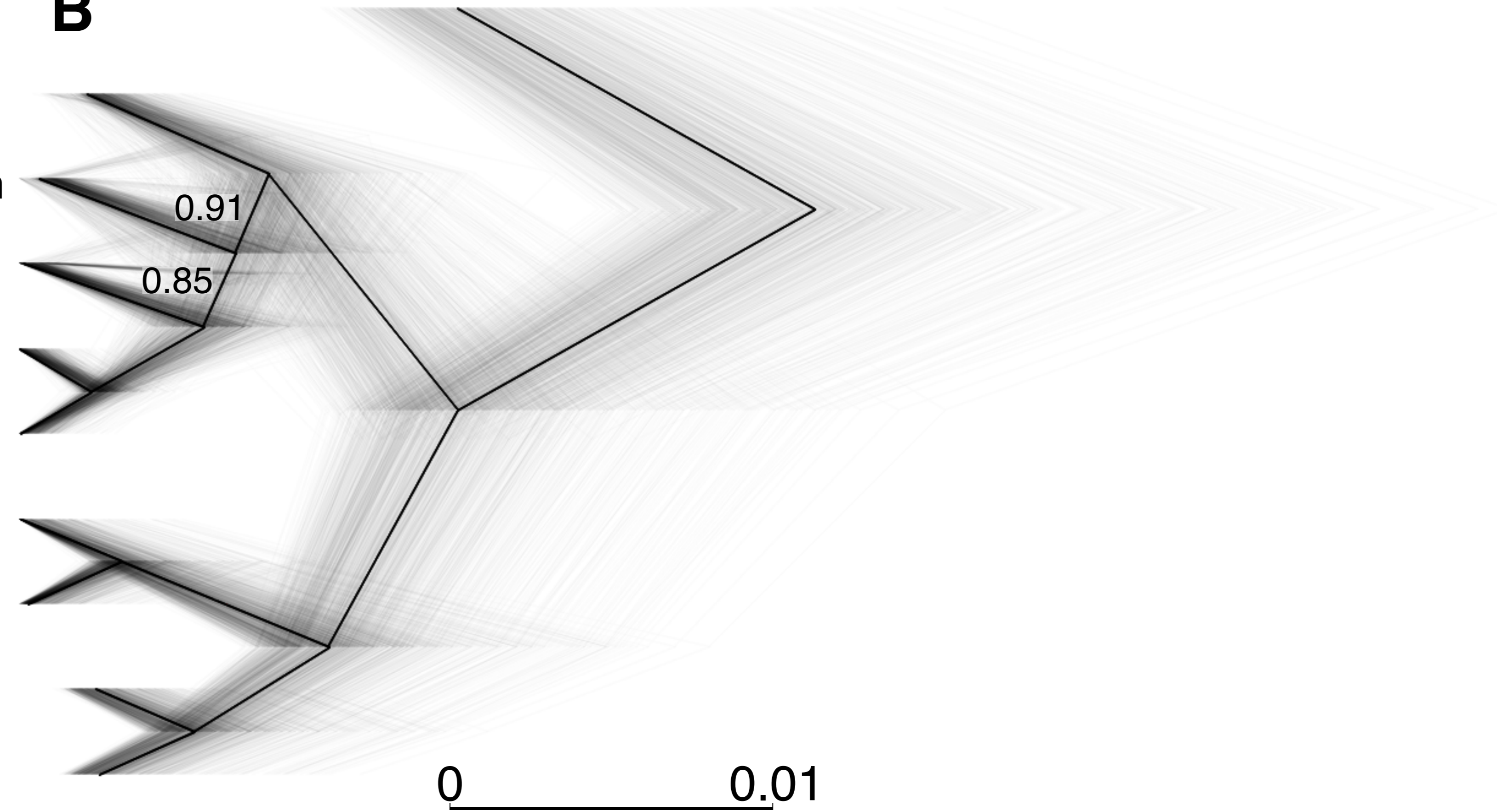
Finless porpoise



Beluga



Narwhal

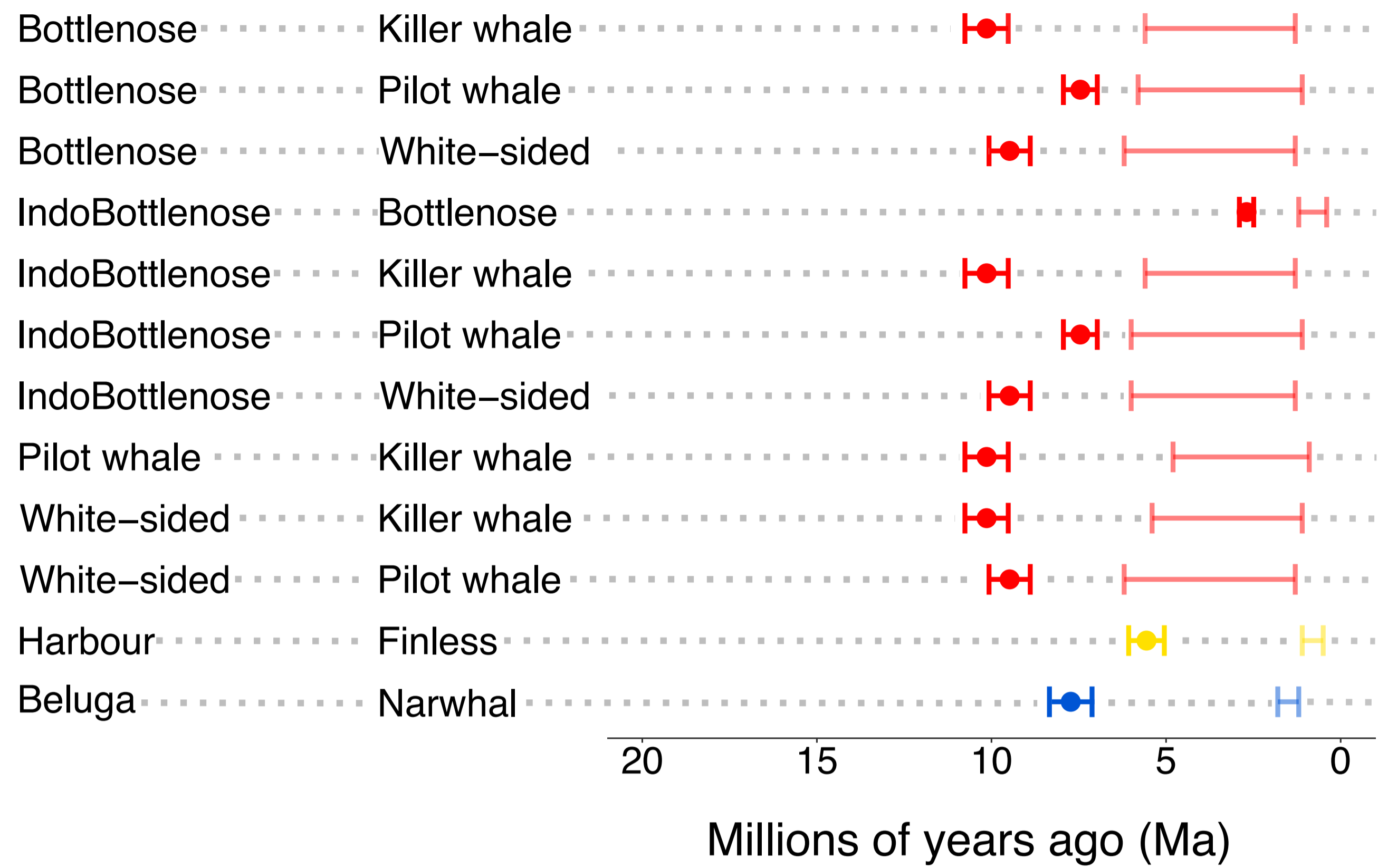
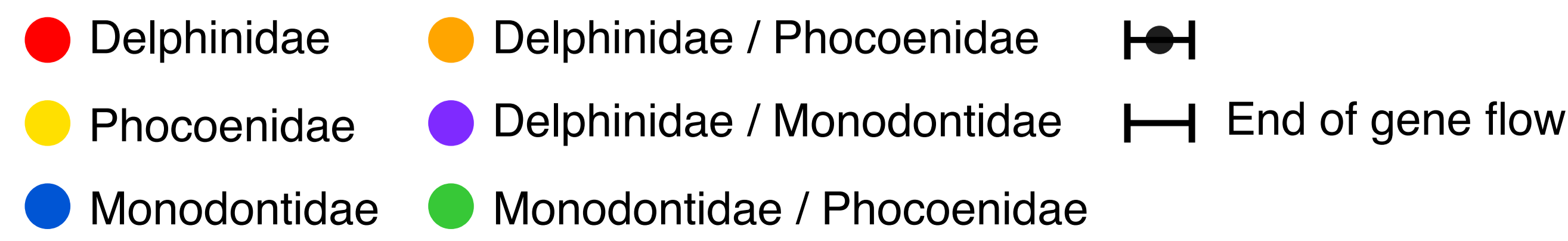
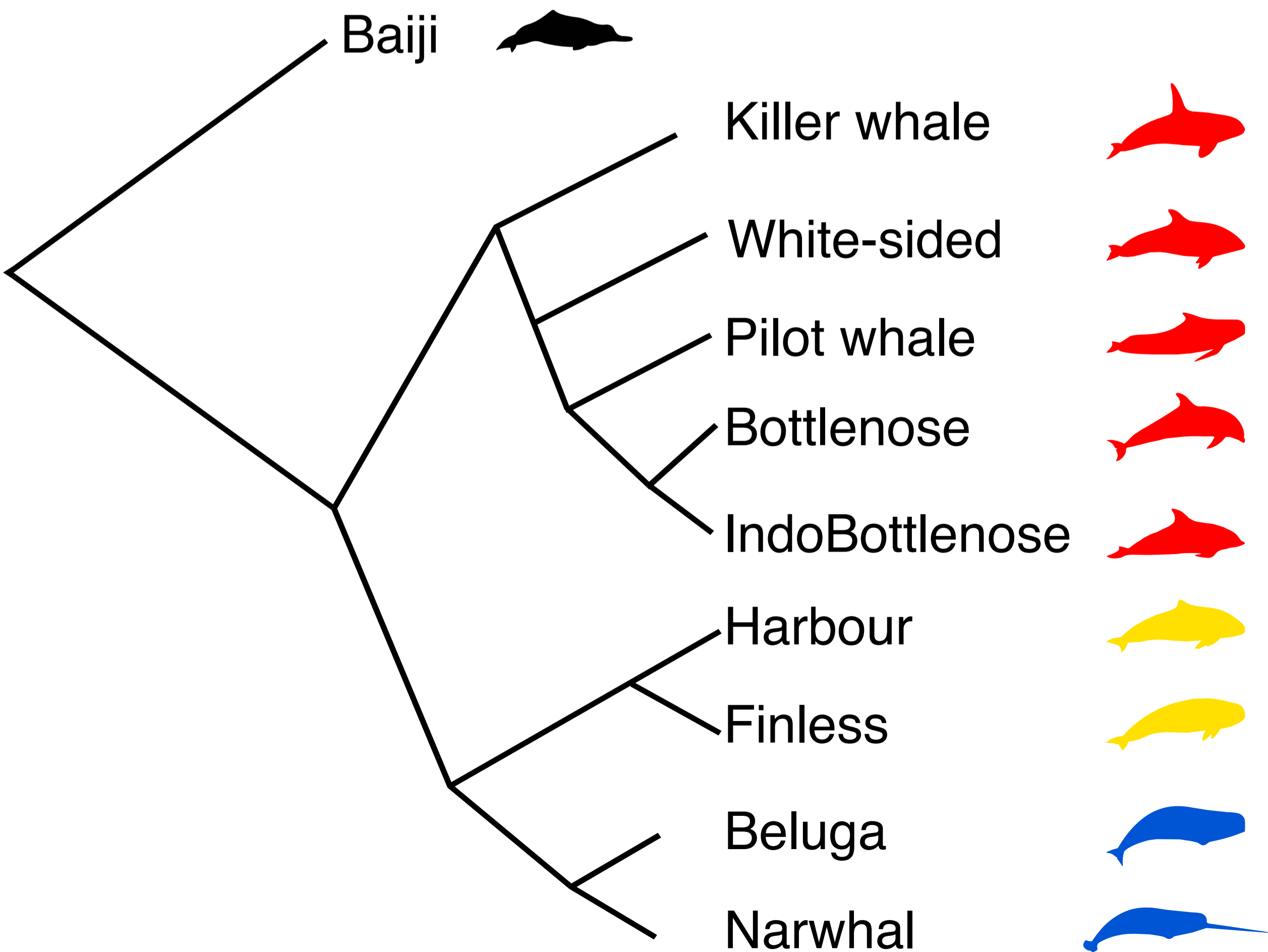
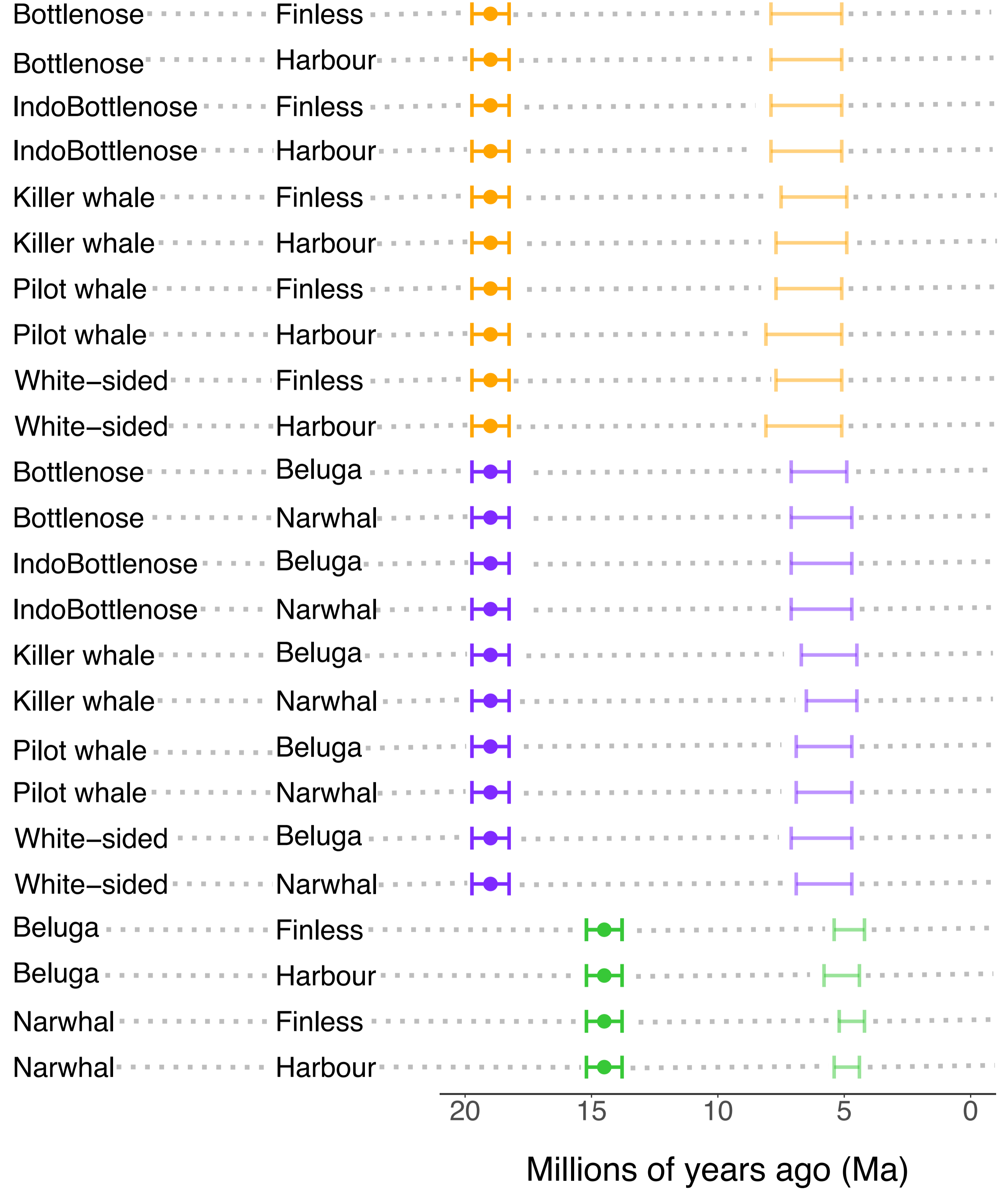
**B**

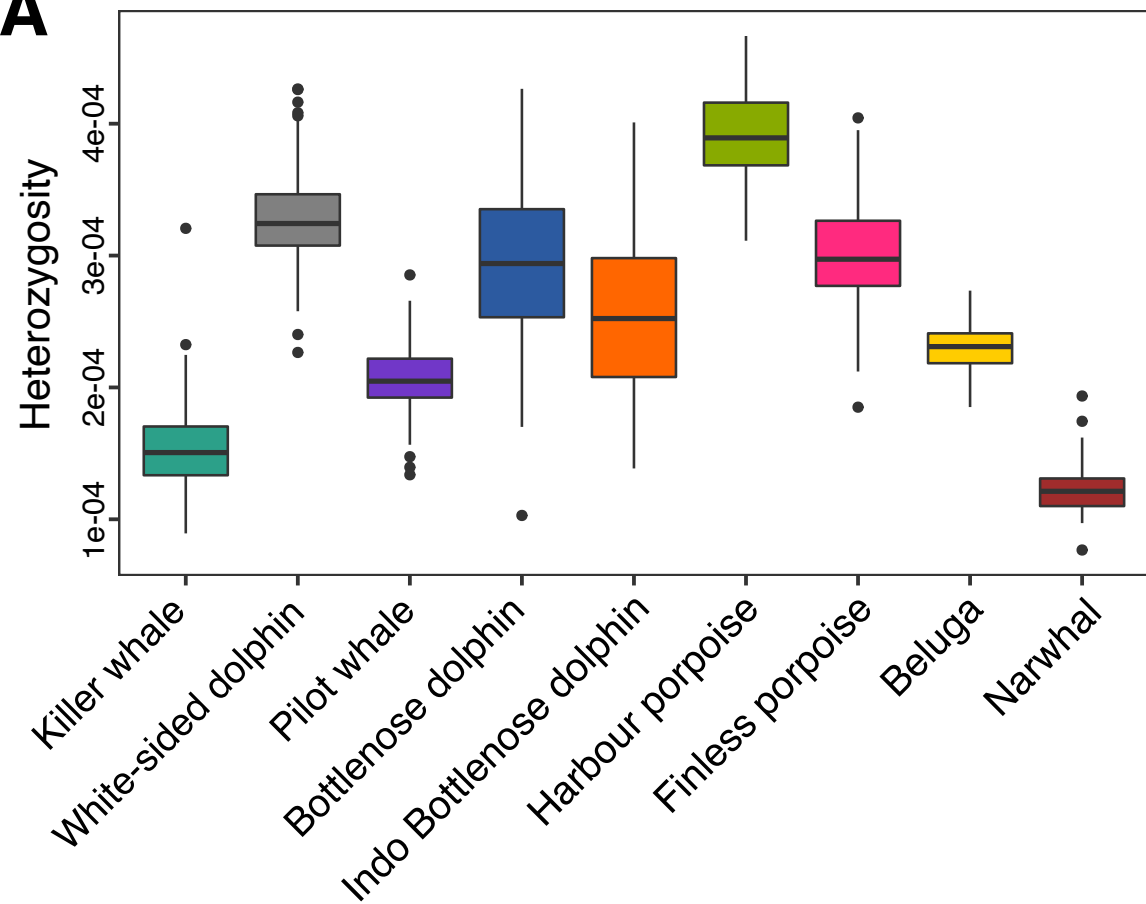
● Outgroup

● Delphinidae

● Phocoenidae



● Monodontidae

**A****B****Between families**

**A****Delphinidae**

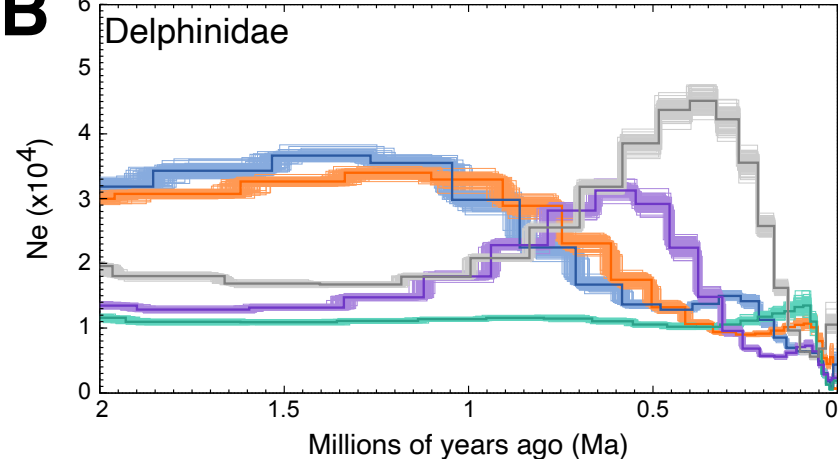
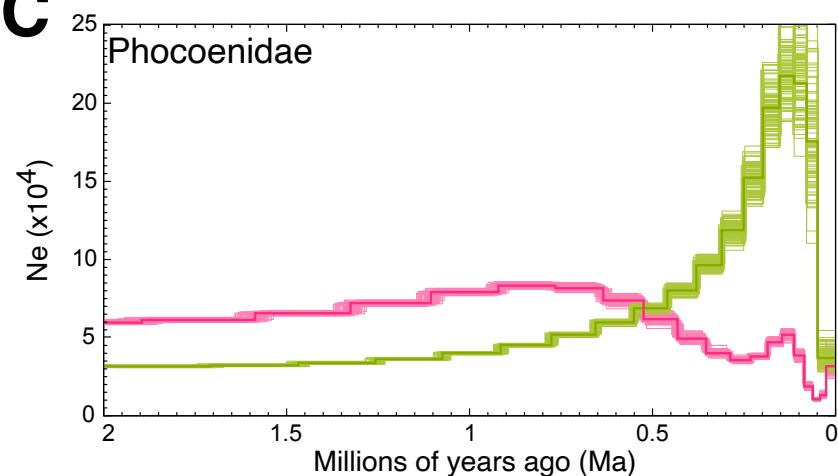
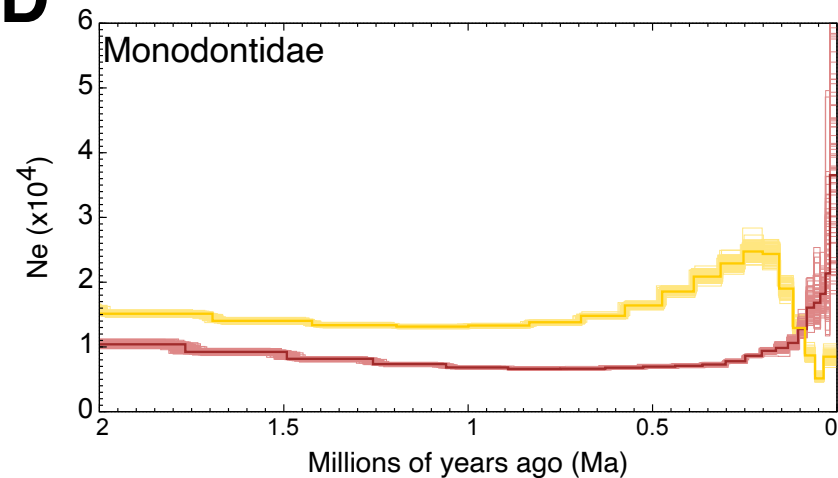
-  Killer whale
-  White-sided dolphin
-  Pilot whale
-  Bottlenose dolphin
-  Indo bottlenose dolphin

**Phocoenidae**

-  Harbour porpoise
-  Finless porpoise

**Monodontidae**

-  Beluga
-  Narwhal

**B****C****D**

## Supplementary information

**Supplementary table S1:** Proportions of the most frequent five topologies based on window sizes. NA - not in the five most frequent for that window size. Whitesided - Pacific white-sided dolphin, Pilotwhale - long-finned pilot whale, IndoBottlenose - Indo-Pacific bottlenose dolphin, Bottlenose - bottlenose dolphin, Killerwhale - killer whale, Beluga - beluga, Narwhal - narwhal, Harbour - harbour porpoise, Finless - finless porpoise, Baiji - Baiji (outgroup).

50kb	100kb	500kb	1Mb	Topology
0.24	0.32	0.64	0.79	(((Whitesided,(Pilotwhale,(IndoBottlenose,Bottlenose))),Killerwhale),(Beluga,Narwhal),(Harbour,Finless)),Baiji);
0.14	0.14	0.09	0.05	(((Pilotwhale,(IndoBottlenose,Bottlenose)),(Whitesided,Killerwhale)),(Beluga,Narwhal),(Harbour,Finless)),Baiji);
0.13	0.14	0.14	0.10	(((Pilotwhale,(Whitesided,(IndoBottlenose,Bottlenose))),Killerwhale),(Beluga,Narwhal),(Harbour,Finless)),Baiji);
0.09	0.08	0.04	0.02	(((Pilotwhale,Whitesided),(IndoBottlenose,Bottlenose)),Killerwhale),(Beluga,Narwhal),(Harbour,Finless)),Baiji);
0.08	NA	NA	NA	(((Killerwhale,(Pilotwhale,(IndoBottlenose,Bottlenose))),Whitesided),(Beluga,Narwhal),(Harbour,Finless)),Baiji);
NA	0.07	0.03	0.02	((Whitesided,((Pilotwhale,(IndoBottlenose,Bottlenose))),Killerwhale),(Beluga,Narwhal),(Harbour,Finless)),Baiji);
0.69	0.76	0.94	0.98	Top 5 topologies combined

**Supplementary table S2:** Proportions of the most frequent five topologies based on GC content and a window size of 50kb. NA - not in the five most frequent for that window size. Whitesided - Pacific white-sided dolphin, Pilotwhale - long-finned pilot whale, IndoBottlenose - Indo-Pacific bottlenose dolphin, Bottlenose - bottlenose dolphin, Killerwhale - killer whale, Beluga - beluga, Narwhal - narwhal, Harbour - harbour porpoise, Finless - finless porpoise, Baiji - Baiji (outgroup).

Low GC	Medium GC	High GC	Topology
2814	3395	4227	(((Killerwhale,(Whitesided,((IndoBottlenose,Bottlenose),Pilotwhale))),((Beluga,Narwhal),(Harbour,Finless))),Baiji);
2023	2107	2085	(((Pilotwhale,(IndoBottlenose,Bottlenose)),(Whitesided,Killerwhale)),(Beluga,Narwhal),(Harbour,Finless)),Baiji);
1740	1898	1976	(((Pilotwhale,(Whitesided,(IndoBottlenose,Bottlenose))),Killerwhale),(Beluga,Narwhal),(Harbour,Finless)),Baiji);
1287	1289	1317	(((Pilotwhale,Whitesided),(IndoBottlenose,Bottlenose)),Killerwhale),(Beluga,Narwhal),(Harbour,Finless)),Baiji);
1152	NA	NA	(((Whitesided,(IndoBottlenose,Bottlenose)),(Pilotwhale,Killerwhale)),(Beluga,Narwhal),(Harbour,Finless)),Baiji);

NA	1190	1149	((Whitesided,((Pilotwhale,(IndoBottlenose,Bottlenose)),Killerwhale)),((Beluga,Narwhal),(Harbour,Finless))),Baiji);
----	------	------	--

**Supplementary table S3:** QuIBL results when using every twentieth tree from the 50kb sliding window analysis - attached as spreadsheet.

**Supplementary table S4:** QuIBL results from trees constructed using 20kb windows with a 1Mb slide - attached as spreadsheet.

**Supplementary table S5:** D-statistics results for all triplet combinations phylogenetically concurrent with our results shown in figure 1. Baiji was used as the outgroup/ancestral sequence. A  $|Z| > 3$  is indicated in bold. Colours indicate the family of the given individual. Red = Delphinidae, yellow = Phocoenidae, blue = Monodontidae.

H1	H2	H3	nABBA	nBABA	D-score	Z-score
Bottlenose	IndoBottlenose	Killer whale	597,251	554,780	0.037	<b>23.26</b>
Bottlenose	IndoBottlenose	Pilotwhale	748,948	691,844	0.040	<b>24.13</b>
Bottlenose	IndoBottlenose	Whitesided	721,498	665,420	0.040	<b>25.20</b>
Pilotwhale	Whitesided	Killer whale	2,224,888	2,119,068	0.024	<b>11.77</b>
Pilotwhale	Bottlenose	Killer whale	1,998,297	1,795,444	0.053	<b>26.15</b>
Pilotwhale	IndoBottlenose	Killer whale	2,004,478	1,757,429	0.066	<b>31.95</b>
Pilotwhale	Bottlenose	Whitesided	2,490,189	2,051,579	0.097	<b>42.67</b>
Pilotwhale	IndoBottlenose	Whitesided	2,508,755	2,007,966	0.111	<b>48.64</b>
Whitesided	Bottlenose	Killer whale	2,111,742	2,014,525	0.024	<b>11.88</b>
Whitesided	IndoBottlenose	Killer whale	2,117,925	1,975,800	0.035	<b>17.25</b>
Killer whale	Pilotwhale	Finless	928,942	840,273	0.050	<b>51.99</b>
Killer whale	Whitesided	Finless	924,323	829,525	0.054	<b>56.12</b>
Killer whale	Pilotwhale	Harbour porpoise	959,748	851,885	0.060	<b>60.74</b>
Killer whale	Whitesided	Harbour porpoise	956,686	840,318	0.065	<b>65.46</b>
Killer whale	Bottlenose	Finless	942,684	757,495	0.109	<b>107.12</b>
Killer whale	Bottlenose	Harbour porpoise	974,032	767,636	0.119	<b>116.98</b>
Killer whale	IndoBottlenose	Finless	943,526	728,185	0.129	<b>120.99</b>
Killer whale	IndoBottlenose	Harbour porpoise	974,967	739,024	0.138	<b>130.60</b>
Pilotwhale	Whitesided	Finless	861,276	855,083	0.004	<b>4.41</b>
Pilotwhale	Whitesided	Harbour porpoise	892,930	884,620	0.005	<b>5.64</b>
Pilotwhale	Bottlenose	Finless	828,193	724,397	0.067	<b>73.75</b>
Pilotwhale	Bottlenose	Harbour porpoise	857,823	749,827	0.067	<b>76.38</b>
Pilotwhale	IndoBottlenose	Finless	829,393	692,413	0.090	<b>97.23</b>
Pilotwhale	IndoBottlenose	Harbour porpoise	859,146	718,044	0.089	<b>98.69</b>

Whitesided	Bottlenose	Harbour porpoise	887,876	787,914	0.060	<b>68.88</b>
Whitesided	Bottlenose	Finless	857,483	760,224	0.060	<b>69.75</b>
Whitesided	IndoBottlenose	Harbour porpoise	888,872	755,955	0.081	<b>92.25</b>
Whitesided	IndoBottlenose	Finless	858,523	727,924	0.082	<b>92.84</b>
Bottlenose	IndoBottlenose	Narwhal	414,272	380,995	0.042	<b>33.84</b>
Bottlenose	IndoBottlenose	Beluga	434,366	396,566	0.045	<b>37.67</b>
Killer whale	Pilotwhale	Narwhal	955,756	837,598	0.066	<b>61.58</b>
Killer whale	Pilotwhale	Beluga	984,462	854,528	0.071	<b>65.67</b>
Killer whale	Whitesided	Narwhal	953,496	826,881	0.071	<b>66.17</b>
Killer whale	Whitesided	Beluga	982,162	844,661	0.075	<b>67.95</b>
Killer whale	Bottlenose	Narwhal	971,164	751,458	0.128	<b>111.86</b>
Killer whale	Bottlenose	Beluga	1,001,546	767,422	0.132	<b>113.69</b>
Killer whale	IndoBottlenose	Narwhal	974,507	722,249	0.149	<b>126.51</b>
Killer whale	IndoBottlenose	Beluga	1,007,582	736,424	0.155	<b>128.87</b>
Pilotwhale	Whitesided	Beluga	918,941	911,423	0.004	<b>4.93</b>
Pilotwhale	Whitesided	Narwhal	891,298	883,114	0.005	<b>5.61</b>
Pilotwhale	Bottlenose	Narwhal	859,652	743,735	0.072	<b>78.60</b>
Pilotwhale	Bottlenose	Beluga	887,196	766,562	0.073	<b>81.55</b>
Pilotwhale	IndoBottlenose	Narwhal	863,608	710,777	0.097	<b>103.83</b>
Pilotwhale	IndoBottlenose	Beluga	895,023	731,826	0.100	<b>105.92</b>
Whitesided	Bottlenose	Narwhal	888,390	780,573	0.065	<b>74.77</b>
Whitesided	Bottlenose	Beluga	917,400	804,237	0.066	<b>76.44</b>
Whitesided	IndoBottlenose	Narwhal	892,496	747,539	0.088	<b>97.69</b>
Whitesided	IndoBottlenose	Beluga	925,091	769,228	0.092	<b>102.86</b>
Finless	Harbour porpoise	Narwhal	452,411	450,657	0.002	1.59
Harbour porpoise	Finless	Beluga	570,767	552,830	0.016	<b>13.47</b>
Narwhal	Beluga	Harbour porpoise	532,605	502,660	0.029	<b>25.72</b>
Narwhal	Beluga	Finless	514,273	466,273	0.049	<b>41.75</b>
Finless	Narwhal	Killer whale	973,140	885,678	0.047	<b>47.30</b>
Finless	Narwhal	Bottlenose	1,077,206	966,370	0.054	<b>55.93</b>
Finless	Narwhal	IndoBottlenose	1,080,812	970,600	0.054	<b>56.63</b>
Finless	Narwhal	Pilotwhale	1,059,846	950,178	0.055	<b>57.27</b>
Finless	Beluga	Killer whale	989,901	875,364	0.061	<b>57.51</b>
Finless	Narwhal	Whitesided	1,062,632	951,040	0.055	<b>57.94</b>
Finless	Beluga	Bottlenose	1,103,352	951,967	0.074	<b>68.54</b>
Finless	Beluga	Pilotwhale	1,084,679	936,511	0.073	<b>68.84</b>
Finless	Beluga	IndoBottlenose	1,109,158	955,589	0.074	<b>69.72</b>

Finless	Beluga	Whitesided	1,087,277	938,148	0.074	<b>69.88</b>
Harbour porpoise	Narwhal	Killer whale	1,004,793	891,909	0.060	<b>59.43</b>
Harbour porpoise	Beluga	Killer whale	1,028,676	885,849	0.075	<b>69.85</b>
Harbour porpoise	Narwhal	Pilotwhale	1,124,641	974,232	0.072	<b>75.43</b>
Harbour porpoise	Narwhal	Bottlenose	1,145,470	990,640	0.072	<b>75.66</b>
Harbour porpoise	Narwhal	Whitesided	1,127,578	976,951	0.072	<b>75.84</b>
Harbour porpoise	Narwhal	IndoBottlenose	1,153,263	994,022	0.074	<b>78.93</b>
Harbour porpoise	Beluga	Pilotwhale	1,163,136	965,266	0.093	<b>88.73</b>
Harbour porpoise	Beluga	Whitesided	1,165,862	968,086	0.093	<b>89.42</b>
Harbour porpoise	Beluga	Bottlenose	1,185,612	981,030	0.094	<b>89.66</b>
Harbour porpoise	Beluga	IndoBottlenose	1,197,547	984,311	0.098	<b>93.10</b>

**Supplementary table S6:** 100kb non-overlapping sliding window D-foil results for all quadruplet combinations [[H1,H2][H3,H4]] phylogenetically concurrent with our results shown in figure 1. Baiji was used as the outgroup/ancestral sequence. - attached as a spreadsheet

**Supplementary table S7:** Mapping statistics of each Delphinoidea species used in this study when specifying the reference genome as the baiji assembly.

Common name	Raw read pairs	Mapped reads	Coverage	Bp-mapped
Beluga	466,374,135	476,814,543	31.44	69,807,010,359
Narwhal	384,563,392	468,429,237	31.09	68,247,058,370
Bottlenose dolphin	578,690,171	732,418,659	47.61	105,524,983,813
Indo-Pacific finless porpoise	523,612,238	557,766,873	24.96	54,450,935,944
Harbour porpoise	289,063,910	418,431,029	23.17	50,830,083,145
Long-finned pilot whale	428,064,233	504,482,080	28.61	63,276,638,573
Indo-Pacific bottlenose dolphin	466,306,082	551,837,703	35.62	78,749,625,267
Pacific white-sided dolphin	453,348,710	499,704,592	28.83	63,800,396,300
Killer whale	1,467,089,287	1,047,260,000	39.53	88,692,400,000



**Supplementary table S8:** Mapping statistics of each Delphinoidea species used in this study when specifying the reference genome as a conspecific assembly.

Common name	Raw read pairs	Mapped reads	Coverage	Bp-mapped
Beluga whale	466,374,135	531,535,936	34.47	79,218,898,913
Narwhal	384,563,392	529,082,769	33.85	78,238,763,386
Bottlenose dolphin	578,690,171	779,210,277	54.03	114,530,169,747
Indo-Pacific finless porpoise	523,612,238	620,580,505	27.33	61,286,732,910
Harbour porpoise	289,063,910	431,762,883	23.74	52,067,455,809
Long-finned pilot whale	428,064,233	598,612,204	32.79	75,639,560,432
Indo-Pacific bottlenose dolphin	466,306,082	587,440,922	37.88	85,032,333,848
Pacific white-sided dolphin	453,348,710	592,814,373	33.02	76,299,243,217
Killer whale	1,467,089,287	1,213,221,913	44.93	100,903,316,971

**Supplementary table S9:** Genome-wide pairwise distance matrix of the nine Delphinoidea included in this study. Bottlenose = bottlenose dolphin, Finless = finless porpoise, Harbour = harbour porpoise, Indobottle = Indo-Pacific bottlenose dolphin, Pilot = pilot whale, White = Pacific whitesided dolphin.

<b>Beluga</b>	0.0000	0.0211	0.0151	0.0153	0.0211	0.0205	0.0056	0.0210	0.0209
<b>Bottlenose</b>	0.0211	0.0000	0.0230	0.0231	0.0040	0.0113	0.0210	0.0102	0.0107
<b>Finless</b>	0.0151	0.0230	0.0000	0.0056	0.0230	0.0224	0.0151	0.0229	0.0228
<b>Harbour</b>	0.0153	0.0231	0.0056	0.0000	0.0231	0.0225	0.0152	0.0231	0.0230
<b>Indobottle</b>	0.0211	0.0040	0.0230	0.0231	0.0000	0.0113	0.0210	0.0102	0.0107
<b>Orca</b>	0.0205	0.0113	0.0224	0.0225	0.0113	0.0000	0.0204	0.0113	0.0112
<b>Narwhal</b>	0.0056	0.0210	0.0151	0.0152	0.0210	0.0204	0.0000	0.0209	0.0208

<b>Pilot</b>	0.0210	0.0102	0.0229	0.0231	0.0102	0.0113	0.0209	0.0000	0.0109
<b>White</b>	0.0209	0.0107	0.0228	0.0230	0.0107	0.0112	0.0208	0.0109	0.0000

**Supplementary table S10:** Metrics used to calculate the mutation rate per year with the equation mutation rate = divergence time / 2x genetic distance. Mean divergences were taken from the full dataset 10-partition AR from McGowen et al 2020 (McGowen et al., 2020) and average genetic distances were calculated from the results shown in supplementary table S5.

<b>Species</b>	<b>Closest relative</b>	<b>Divergence (Ma)</b>	<b>Distance</b>	<b>Mutation rate per year</b>
<i>Delphinapterus leucas</i>	<i>Monodon monoceros</i>	7.72	0.0056	3.63x10 <sup>-10</sup>
<i>Orcinus orca</i>	Delphinidae	10.16	0.0113	5.56x10 <sup>-10</sup>
<i>Tursiops truncatus</i>	<i>Tursiops aduncus</i>	2.69	0.0040	7.51x10 <sup>-10</sup>
<i>Phocoena phocoena</i>	<i>Neophocaena phocaenoides</i>	5.36	0.0056	5.25x10 <sup>-10</sup>
<i>Globicephala melas</i>	<i>Tursiops spp.</i>	7.46	0.0102	6.83x10 <sup>-10</sup>
<i>Lagenorhynchus obliquidens</i>	<i>Tursiops + Globicephala</i>	9.48	0.0108	5.69x10 <sup>-10</sup>

**Supplementary table S11:** Generation times, generational mutation rates and references for the generation times for each of the nine Delphinoidea species used in this study.

<b>Common name</b>	<b>Generation time</b>	<b>Generational mutation rate</b>	<b>Generation time reference</b>
Beluga	32	1.16x10 <sup>-8</sup>	(Garde et al., 2015)
Narwhal	30	1.09x10 <sup>-8</sup>	(Garde et al., 2015)
Killer whale	25.7	1.43x10 <sup>-8</sup>	(Foote et al., 2016)
Bottlenose dolphin	21	1.58x10 <sup>-8</sup>	(Taylor et al., 2007)
Indo-Pacific finless porpoise	8	4.20x10 <sup>-9</sup>	(Zhou et al., 2018)
Harbour porpoise	10	5.25x10 <sup>-9</sup>	(Birkun and Frantzis, 2008)
Long-finned pilot whale	24	1.64x10 <sup>-8</sup>	(Taylor et al., 2007)

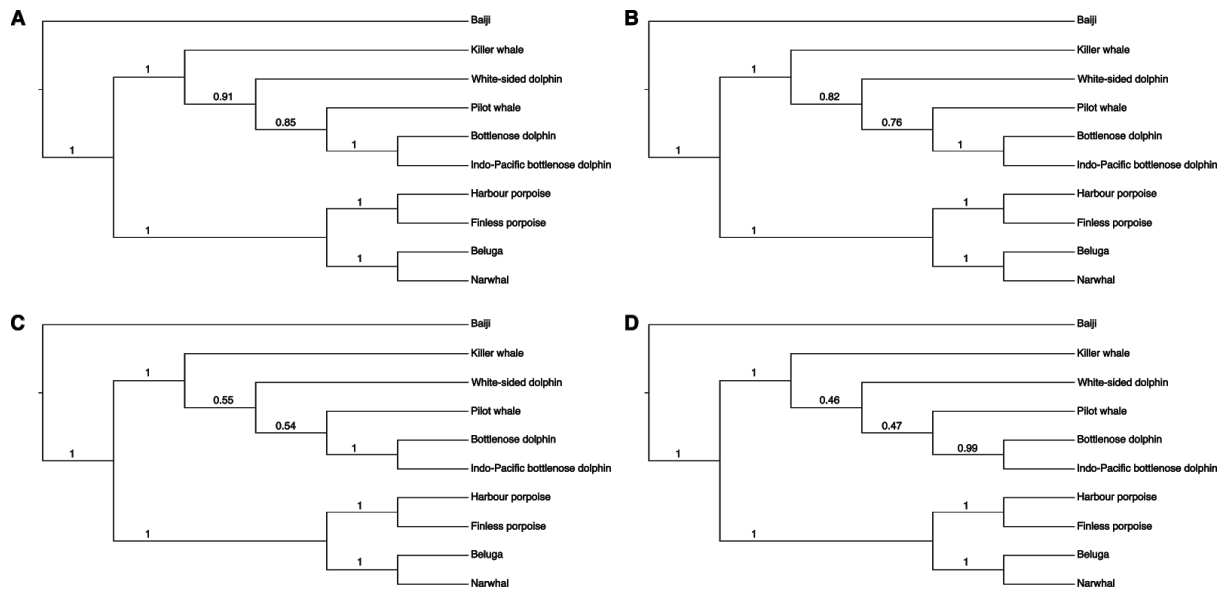
Indo-Pacific bottlenose dolphin	21	$1.58 \times 10^{-8}$	(Taylor et al., 2007)
Pacific white-sided dolphin	21.2	$1.21 \times 10^{-8}$	(Taylor et al., 2007)

**Supplementary table S12:** The pre-divergence  $N_e$ , divergence time intervals, and the increments specified for each of the species pair used for the simulations to compare against the hPSMC results.

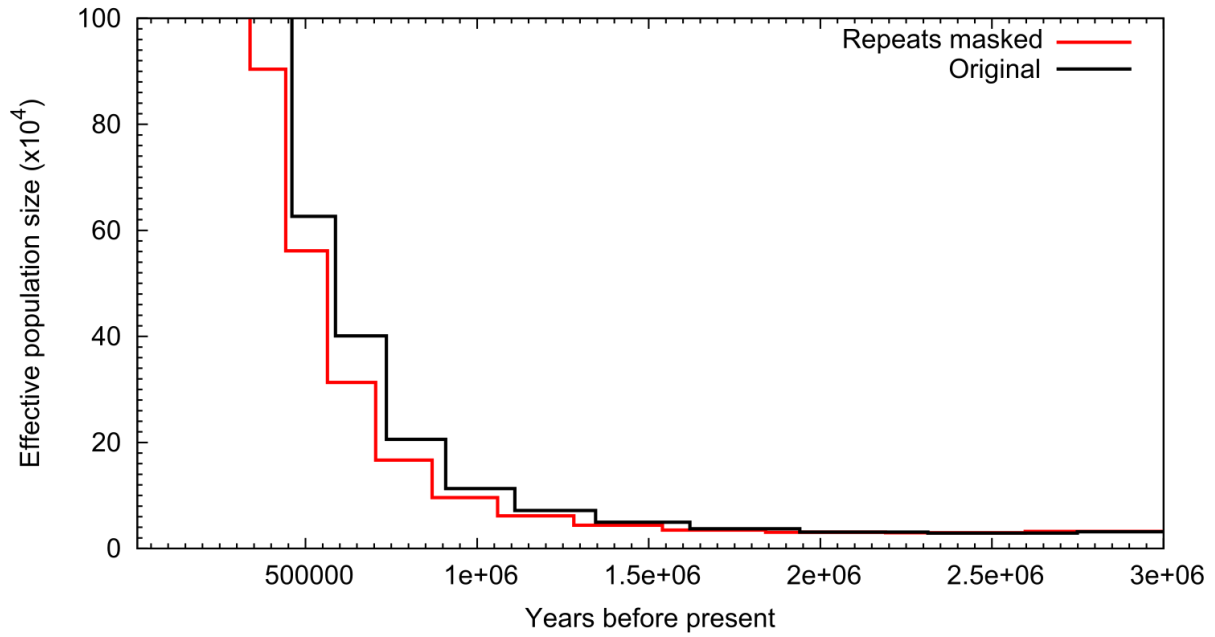
Species pair	Pre-divergence $N_e$	Range (Ma)	Increments (years)
Beluga whale + Narwhal	30,000	1-2	100,000
Beluga whale + Finless porpoise	60,000	3-7	200,000
Beluga whale + Harbour porpoise	60,000	3-7	200,000
Narwhal + Finless porpoise	60,000	3-7	200,000
Narwhal + Harbour porpoise	60,000	3-7	200,000
Beluga whale + Bottlenose dolphin	105,000	3.9-8.5	200,000
Beluga whale + Indo-Pacific bottlenose dolphin	105,000	3.9-8.5	200,000
Narwhal + Bottlenose dolphin	105,000	3.9-8.5	200,000
Narwhal + Indo-Pacific bottlenose dolphin	105,000	3.9-8.5	200,000
Narwhal + Killer whale	105,000	3.9-8.5	200,000
Narwhal + Long-finned pilot whale	105,000	3.9-8.5	200,000
Narwhal + Pacific white-sided dolphin	105,000	3.9-8.5	200,000
Beluga whale + Killer whale	105,000	3.9-8.5	200,000
Beluga whale + Long-finned pilot whale	105,000	3.9-8.5	200,000
Beluga whale + Pacific white-sided dolphin	105,000	3.9-8.5	200,000
Harbour porpoise + Bottlenose dolphin	105,000	3.9-8.5	200,000
Harbour porpoise + Indo-Pacific bottlenose dolphin	105,000	3.9-8.5	200,000
Finless porpoise + Bottlenose dolphin	105,000	3.9-8.5	200,000
Finless porpoise + Indo-Pacific bottlenose dolphin	105,000	3.9-8.5	200,000
Finless porpoise + Killer whale	105,000	3.9-8.5	200,000
Finless porpoise + Long-finned pilot whale	105,000	3.9-8.5	200,000

Finless porpoise + Pacific white-sided dolphin	105,000	3.9-8.5	200,000
Harbour porpoise + Killer whale	105,000	3.9-8.5	200,000
Harbour porpoise + Long-finned pilot whale	105,000	3.9-8.5	200,000
Harbour porpoise + Pacific white-sided dolphin	105,000	3.9-8.5	200,000
Harbour porpoise + Finless porpoise	40,000	0.3-1.4	100,000
Indo-Pacific Bottlenose dolphin + Bottlenose dolphin	20,000	0.2-1.2	100,000
Indo-Pacific bottlenose dolphin + Killer whale	50,000	0.9-2.1 & 3.4-7	200,000
Indo-Pacific bottlenose dolphin + Long-finned pilot whale	50,000	0.9-2.1 & 3.4-7	200,000
Indo-Pacific bottlenose dolphin + Pacific white-sided dolphin	50,000	0.9-2.1 & 3.4-7	200,000
Bottlenose dolphin + Killer whale	50,000	0.9-2.1 & 3.4-7	200,000
Bottlenose dolphin + Long-finned pilot whale	50,000	0.9-2.1 & 3.4-7	200,000
Bottlenose dolphin + Pacific white-sided dolphin	50,000	0.9-2.1 & 3.4-7	200,000
Long-finned pilot whale + Killer whale	60,000	0.9-2.1 & 3.4-7	200,000
Pacific white-sided dolphin + Killer whale	50,000	0.9-2.1 & 3.4-7	200,000
Pacific white-sided dolphin + Long-finned pilot whale	50,000	0.9-2.1 & 3.4-7	200,000

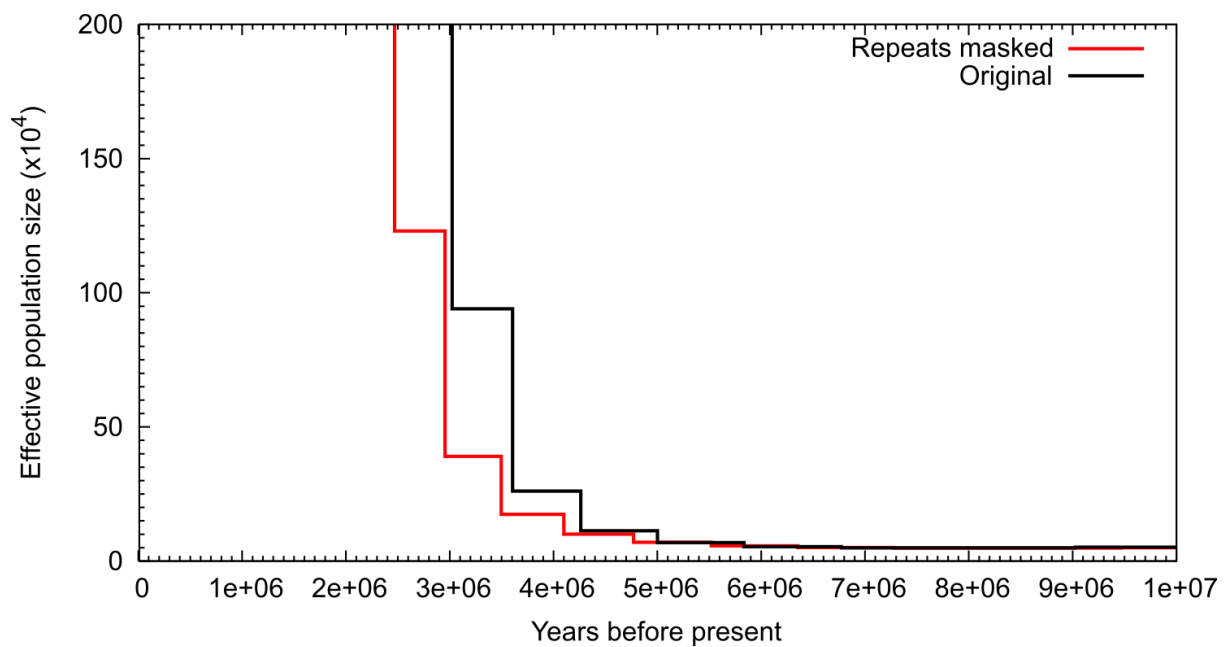
## Supplementary figures



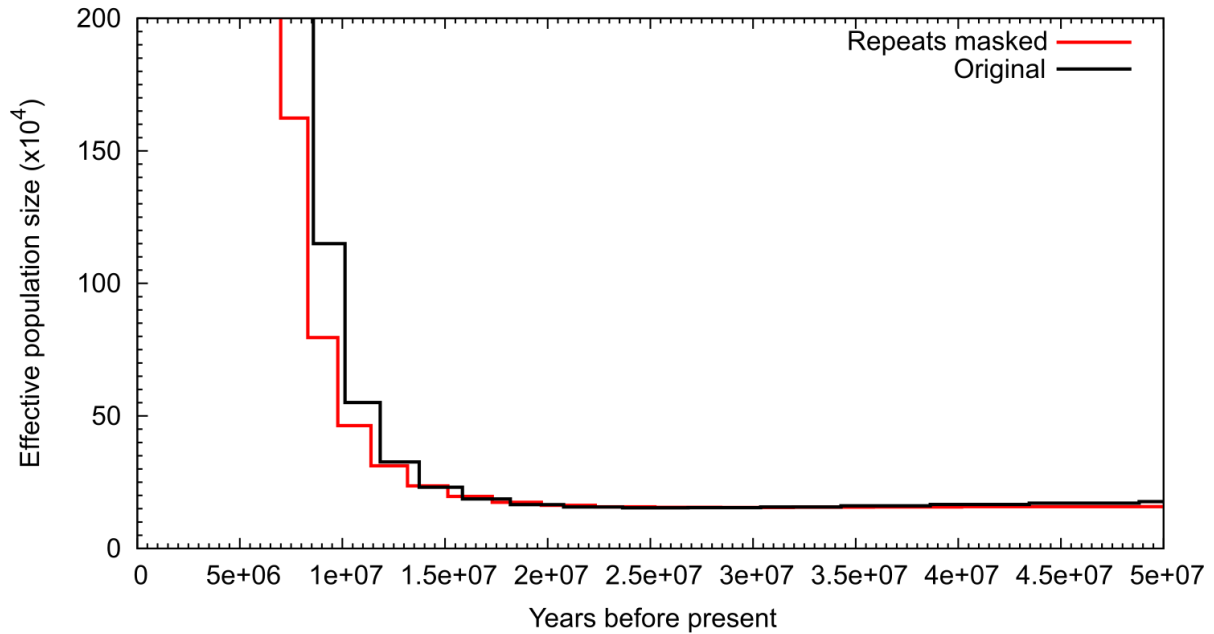
**Supplementary figure S1:** Consensus trees of independent Maximum-Likelihood trees constructed from non-overlapping sliding windows of (A) 1Mb, (B) 500kb, (C) 100kb, or (D) 50kb in length. Branch numbers represent the number of independent trees supporting each node.



**Supplementary figure S2:** Comparison of hPSMC results using a pseudodiploid sequence from the bottlenose and Indo-Pacific bottlenose dolphins (shallow divergence) with either repeat regions masked or not.



**Supplementary figure S3:** Comparison of hPSMC results using a pseudodiploid sequence from the beluga and narwhal (medium divergence) with either repeat regions masked or not.



**Supplementary figure S4:** Comparison of hPSMC results using a pseudodiploid sequence from the bottlenose dolphin and beluga (deep divergence) with either repeat regions masked or not.

### Supplementary results

Additional plots of the hPSMC empirical and simulated data can be found under the following link: [https://sid.erda.dk/cgi-sid/lis.py?share\\_id=ewvczfS2hH](https://sid.erda.dk/cgi-sid/lis.py?share_id=ewvczfS2hH) on the University of Copenhagen's electronic research data archive (ERDA). Bold lines show the hPSMC empirical data, faded lines show the simulated data, and the black lines show the simulated data that most closely match the empirical data without overlapping it between 1.5x and 10x the pre-divergence  $N_e$ .

## Supplementary references

- Birkun AA Jr, Frantzis A. 2008. *Phocoena phocoena* ssp. *relicta*. *The IUCN Red List of Threatened Species [Internet]*.
- Footo AD, Vijay N, Ávila-Arcos MC, Baird RW, Durban JW, Fumagalli M, Gibbs RA, Hanson MB, Korneliussen TS, Martin MD, Robertson KM, Sousa VC, Vieira FG, Vinař T, Wade P, Worley KC, Excoffier L, Morin PA, Gilbert MTP, Wolf JBW. 2016. Genome-culture coevolution promotes rapid divergence of killer whale ecotypes. *Nat Commun* 7:11693.
- Garde E, Hansen SH, Ditlevsen S, Tvermosegaard KB, Hansen J, Harding KC, Heide-Jørgensen MP. 2015. Life history parameters of narwhals (*Monodon monoceros*) from Greenland. *J Mammal* 96:866–879.
- McGowen MR, Tsagkogeorga G, Álvarez-Carretero S, Dos Reis M, Struebig M, Deaville R, Jepsen PD, Jarman S, Polanowski A, Morin PA, Rossiter SJ. 2020. Phylogenomic Resolution of the Cetacean Tree of Life Using Target Sequence Capture. *Syst Biol* 69:479–501.
- Taylor BL, Chivers SJ, Larese J, Perrin WF. 2007. Generation length and percent mature estimates for IUCN assessments of cetaceans (No. Administrative Report LJ-07-01 ). National Marine Fisheries Service, Southwest Fisheries Science Center.
- Zhou X, Guang X, Sun D, Xu S, Li M, Seim I, Jie W, Yang L, Zhu Q, Xu J, Gao Q, Kaya A, Dou Q, Chen B, Ren W, Li S, Zhou K, Gladyshev VN, Nielsen R, Fang X, Yang G. 2018. Population genomics of finless porpoises reveal an incipient cetacean species adapted to freshwater. *Nat Commun* 9:1276.



Triplet analysed	Geneflow pair	outgroup	Proportion of windows with gene flow	BIC2Dist (IBS + Geneflow)	BIC1Dist (IBS alone)	BIC difference	Significant for gene flow (BIC difference <10)	Number of trees	Percentage of total trees (2161) from triplet	Percentage of trees supporting topology explained by gene flow
Indo-Pacific Bottlenose dolphin_Bottlenose dolphin_K	Bot-Orca	Indo-Pacific Bottlenose	1	-47.1718	-40.833	-6.34	No	4	0.19	1.09
Pilot whale_Bottlenose dolphin_Killer whale	Bot-Orca	Pilot whale	0.994524	-4176.75	-4015.52	-161.23	Yes	363	16.80	44.13
White-sided dolphin_Bottlenose dolphin_Killer whale	Bot-Orca	White-sided dolphin	0.932662	-5203	-5001.75	-201.25	Yes	451	20.87	51.55
Indo-Pacific Bottlenose dolphin_Bottlenose dolphin_K	Indo-Orca	Bottlenose dolphin	1	-35.0559	-32.055	-3.00	No	3	0.14	0.37
Pilot whale_Indo-Pacific Bottlenose dolphin_Killer whale	Indo-Orca	Pilot whale	0.994149	-4163.39	-4003.35	-160.04	Yes	362	16.75	44.27
White-sided dolphin_Indo-Pacific Bottlenose dolphin_K	Indo-Orca	White-sided dolphin	0.936622	-5157.77	-4961.79	-195.98	Yes	448	20.73	91.82
Pilot whale_Indo-Pacific Bottlenose dolphin_Bottlenose dolphin	Pilot-Bot	Indo-Pacific Bottlenose	1	-56.1656	-53.3674	-2.80	No	5	0.23	1.09
Pilot whale_Indo-Pacific Bottlenose dolphin_Bottlenose dolphin	Pilot-Indo	Bottlenose dolphin	0.26425	-43.6088	-44.5198	0.91	No	4	0.19	0.15
Pilot whale_Bottlenose dolphin_Killer whale	Pilot-Orca	Bottlenose dolphin	0.89395	-4149.09	-3995.26	-153.83	Yes	353	16.34	26.63
Pilot whale_Indo-Pacific Bottlenose dolphin_Killer whale	Pilot-Orca	Indo-Pacific Bottlenose	0.894701	-4145.01	-3991.4	-153.61	Yes	353	16.34	24.46
White-sided dolphin_Pilot whale_Killer whale	Pilot-Orca	White-sided dolphin	0.890091	-5551.99	-5354.47	-197.52	Yes	479	22.17	30.52
White-sided dolphin_Pilot whale_Bottlenose dolphin	Pilot-White	Bottlenose dolphin	0.885824	-5329.17	-5126.07	-203.10	Yes	459	21.24	44.05
White-sided dolphin_Pilot whale_Indo-Pacific Bottlenose dolphin	Pilot-White	Indo-Pacific Bottlenose	0.883297	-5332.08	-5127.41	-204.67	Yes	459	21.24	37.09
White-sided dolphin_Indo-Pacific Bottlenose dolphin_Killer whale	White-Bot	Indo-Pacific Bottlenose	0.99938	-53.2849	-53.8868	0.60	No	5	0.23	0.46
White-sided dolphin_Pilot whale_Bottlenose dolphin	White-Bot	Pilot whale	0.870174	-7160.67	-6929.73	-230.94	Yes	629	29.11	86.33
White-sided dolphin_Indo-Pacific Bottlenose dolphin_Killer whale	White-Indo	Bottlenose dolphin	0.859332	-41.6525	-42.3186	0.67	No	4	0.19	0.31
White-sided dolphin_Pilot whale_Indo-Pacific Bottlenose dolphin	White-Indo	Pilot whale	0.871914	-7154.12	-6919.18	-234.94	Yes	628	29.06	49.33
White-sided dolphin_Bottlenose dolphin_Killer whale	White-Orca	Bottlenose dolphin	0.974941	-5679.95	-5365.25	-314.70	Yes	478	22.12	29.40
White-sided dolphin_Indo-Pacific Bottlenose dolphin_Killer whale	White-Orca	Indo-Pacific Bottlenose	0.975064	-5687.27	-5373.09	-314.18	Yes	479	22.17	31.43
White-sided dolphin_Pilot whale_Killer whale	White-Orca	Pilot whale	0.953523	-6205.88	-5910.93	-294.95	Yes	529	24.48	50.04

Triplet analysed	Geneflow pair	outgroup	Proportion of windows with gene flow	BIC2Dist (IBS + Geneflow)	BIC1Dist (IBS alone)	BIC difference	Significant for gene flow (BIC difference <10)	Number of trees	Percentage of total trees (2730) from triplet	Percentage of trees supporting topology explained by gene flow
Indo-Pacific Bottlenose dolphin_Bottlenose dolphin_Killer whale	Bot-Orca	Indo-Pacific Bottl	0.82	-143.55	-144.83	1.28	No	13	0.48	0.39
Pilot whale_Bottlenose dolphin_Killer whale	Bot-Orca	Pilot whale	0.64	-5877.09	-5828.01	-49.08	Yes	543	19.89	12.79
White-sided dolphin_Bottlenose dolphin_Killer whale	Bot-Orca	White-sided dolp	0.68	-6493.50	-6410.93	-82.57	Yes	589	21.58	14.76
Indo-Pacific Bottlenose dolphin_Bottlenose dolphin_Killer whale	Indo-Orca	Bottlenose dolph	0.85	-82.72	-81.61	-1.11	No	8	0.29	0.25
Pilot whale_Indo-Pacific Bottlenose dolphin_Killer whale	Indo-Orca	Pilot whale	0.67	-5836.61	-5777.56	-59.05	Yes	539	19.74	13.24
White-sided dolphin_Indo-Pacific Bottlenose dolphin_Killer whale	Indo-Orca	White-sided dolp	0.69	-6501.26	-6417.36	-83.90	Yes	590	21.61	14.82
Pilot whale_Indo-Pacific Bottlenose dolphin_Bottlenose dolphin	Pilot-Bot	Indo-Pacific Bottl	0.80	-306.79	-305.15	-1.64	No	28	1.03	0.82
Pilot whale_Indo-Pacific Bottlenose dolphin_Bottlenose dolphin	Pilot-Indo	Bottlenose dolph	0.46	-330.52	-336.87	6.35	No	31	1.14	0.52
Pilot whale_Bottlenose dolphin_Killer whale	Pilot-Orca	Bottlenose dolph	0.48	-5643.28	-5648.29	5.01	No	521	19.08	9.13
Pilot whale_Indo-Pacific Bottlenose dolphin_Killer whale	Pilot-Orca	Indo-Pacific Bottl	0.51	-5701.86	-5699.31	-2.55	No	525	19.23	9.77
Pilot whale_White-sided dolphin_Killer whale	Pilot-Orca	White-sided dolp	0.55	-6892.35	-6861.90	-30.45	Yes	631	23.11	12.75
Pilot whale_White-sided dolphin_Bottlenose dolphin	Pilot-White	Bottlenose dolph	0.59	-7033.39	-6989.18	-44.21	Yes	648	23.74	14.00
Pilot whale_White-sided dolphin_Indo-Pacific Bottlenose dolphin	Pilot-White	Indo-Pacific Bottl	0.59	-7073.33	-7026.60	-46.73	Yes	651	23.85	14.15
Pilot whale_White-sided dolphin_Bottlenose dolphin	White-Bot	Pilot whale	0.51	-9197.44	-9186.93	-10.51	Yes	865	31.68	16.05
White-sided dolphin_Indo-Pacific Bottlenose dolphin_Bottlenose d	White-Bot	Indo-Pacific Bottl	0.63	-257.04	-258.27	1.24	No	24	0.88	0.56
Pilot whale_White-sided dolphin_Indo-Pacific Bottlenose dolphin	White-Indo	Pilot whale	0.49	-9117.94	-9115.68	-2.26	No	858	31.43	15.41
White-sided dolphin_Indo-Pacific Bottlenose dolphin_Bottlenose d	White-Indo	Bottlenose dolph	0.40	-170.67	-176.49	5.81	No	16	0.59	0.23
Pilot whale_White-sided dolphin_Killer whale	White-Orca	Pilot whale	0.67	-8498.20	-8408.06	-90.14	Yes	784	28.72	19.25
White-sided dolphin_Bottlenose dolphin_Killer whale	White-Orca	Bottlenose dolph	0.75	-7986.93	-7853.23	-133.70	Yes	726	26.59	19.83
White-sided dolphin_Indo-Pacific Bottlenose dolphin_Killer whale	White-Orca	Indo-Pacific Bottl	0.75	-7983.67	-7846.07	-137.60	Yes	726	26.59	20.03

